3. EXPLANATORY NOTES[1]

Shipboard Scientific Party[2]

INTRODUCTION

Standard procedures for both drilling operations and preliminary shipboard analysis of the material recovered during Deep Sea Drilling Project (DSDP) and Ocean Drilling Program (ODP) drilling have been regularly amended and upgraded since drilling began in 1968. In this chapter we have assembled information that will help the reader understand the basis for our preliminary conclusions and also help the interested investigator select samples for further analysis. This information concerns only shipboard operations and analyses described in the site reports in the *Initial Reports* of the Leg 122 *Proceedings of the Ocean Drilling Program*. Methods used by various investigators for shore-based analysis of Leg 122 data will be detailed in the individual scientific contributions published in the *Scientific Results* volume.

The Leg 122 *Initial Reports* volume is organized with an introductory section containing the following chapters: "Summary and Highlights of Leg 122," "Introduction", "Explanatory Notes," and "Underway Geophysics." This section is then followed by the individual site chapters.

AUTHORSHIP OF SITE CHAPTERS

Authorship of the site report is shared among the entire shipboard scientific party, although the two Co-Chief scientists and the staff scientist edited and rewrote part of the material prepared by other individuals. The site chapters are organized as follows (authors are listed in alphabetical order in parentheses; no seniority is implied):

Site Summary (Haq, von Rad)
Background and Objectives (Haq, von Rad)
Operations (Hanson, O'Connell)
Lithostratigraphy (Borella, Boyd, Dumont, Exon, Görür, Ito, Moxon, O'Connell, Sarti)
Biostratigraphy (Blome, Bralower, Brenner, Oda, Siesser, Wonders)
Paleomagnetics (Galbrun, Tang)
Inorganic Geochemistry (De Carlo)
Organic Geochemistry (Meyers, Snowdon)
Physical Properties (Bent, Boyd, Lorenzo, O'Brien)
Logging (Golovchenko, Wilkens)
Seismic Stratigraphy (Williamson, Exon, Haq, Boyd)
Summary and Conclusions (Haq, von Rad)

Summary core descriptions ("barrel sheets") and photographs of each core appear at the end of the volume.

DEFINITIONS

Many terms in this volume are used either in a format unfamiliar to the reader or different from previous DSDP-ODP format. In order to make these terms more readily understandable they are defined in this section.

Conventional Use of Time and Time-Rock Units

The subdivisions of epochs and series into early, middle, and late, or lower, middle, and upper have no real formal standing in stratigraphy. The subdivision of lithostratigraphic (rock), chronostratigraphic (time-rock), and the geochronologic (time) units, is effected throughout this volume as follows.

Lithostratigraphic Units

For rock units, the terms *lower*, *middle*, and *upper* (i.e., lowercase) are used to subdivide strata (i.e., formations, or other sections of rocks) on the basis of superposition only and thus do not imply time-partitioning.

Chronostratigraphic Units

These units imply bodies of strata formed during specific intervals of geologic time. According to convention they are subdivided using *lower*, *middle*, and *upper*. The bases of formal time-rock units are stages, each of which has, or should have, a stratotype (i.e., a standard section with which other sections can be compared). Stages are conventionally grouped into subunits that subdivide the series. For Leg 122, when referring to the entire subdivision of the series we capitalized *L*ower, *M*iddle, and *U*pper. Otherwise, lower, middle, and upper (i.e., lowercase) were used when referring to only a portion of the subunit (or its equivalent), or when using the subunit in the informal sense.

Geochronologic Units

When speaking of time, age, or of sections in the temporal sense, *early*, *middle*, and *late* are used for subdivision. The bases of the formal geochronologic units are ages (the time equivalent of stages). Like stages, ages are grouped to form the time subunits that subdivide epochs. When speaking of the entire subunit we capitalized *E*arly, *M*iddle, and *L*ate; are capitalized, but not when referring to only a part of the subunit, or when using the subunit in the informal sense. However, such combinations as *e*arly *E*arly, *m*iddle *E*arly, *l*ate *E*arly, etc., were used when older, medial, or younger parts of the entire subunit are implied.

Sequence Stratigraphic Terminology

The documentation of cycles of sea-level change on Exmouth Plateau was one of the major objectives of Leg 122. To accomplish this, sequence stratigraphic analyses of the cores, well logs, and seismic units were conducted on the Leg 122 continental margin sections. Key concepts related to depositional sequences are defined and explained below as in Haq et al. (1987), Posamentier et al. (1988), and Van Wagoner et al. (1988).

[1] Haq, B. U., von Rad, U., et al., 1990. *Proc. ODP, Init. Repts.*, 122: College Station, TX (Ocean Drilling Program).

[2] Shipboard Scientific Party is as given in the list of Participants preceding the contents.

Sequence Stratigraphy

Sequence stratigraphy is the aspect of stratigraphy that deals with depositional sequences of genetically related strata deposited during the different phases (lowstand, transgressive, and highstand) of sea-level cycles.

Sequence

A *sequence* is a relatively conformable succession of genetically related strata bounded at the base and top by unconformities or their correlative conformities (*sequence boundaries*). It is composed of a succession of systems tracts deposited during a cycle of sea-level change (a complete cycle = sea-level fall, succeeded by a rise, and followed by a subsequent fall). Sequence boundaries can be *Type 1* unconformities, produced as a result of rapid sea-level falls that expose the shelf, or *Type 2* unconformities, formed after slower sea-level falls, at which time the whole shelf may not be exposed (Fig. 1).

Systems Tracts

Systems tracts are linkages of contemporaneous depositional systems; depositional systems are defined as genetically linked, three-dimensional assemblages of lithofacies (Brown and Fisher, 1977). Each systems tract is associated with a specific phase of the sea-level cycle as follows: lowstand systems tract, transgressive systems tract, highstand systems tract, and shelf-margin systems tract (the latter is analogous to lowstand systems tract, but deposited above a Type 2 sequence boundary marked by a Type 2 unconformity; see Fig. 1).

Depositional Surfaces

Depositional surfaces separate systems tracts that can be distinguished in outcrops, cores, well logs, and seismic lines by the recognition of three distinct surfaces:

1. *Sequence boundary:* is expressed either as an obvious unconformity or by more subtle changes, depending on the position of the section along the shelf-to-basin profile. On seismic lines it is expressed by the downward (basinward) shift of coastal onlap.
2. *Transgressive surface:* occurs above lowstand deposits (sediments of the regressive phase) and is commonly marked by prominent lithologic changes associated with the sea-level rise (e.g., from relatively shallower to deeper facies). In the absence of lowstand deposits, the transgressive surface may coincide the with underlying sequence boundary.
3. *Downlap surface:* is associated with maximum flooding of the shelf and the formation of the condensed section (see below).

Condensed Section

A *condensed section* is an interval of depositional starvation on the middle-to-outer shelf and slope formed when rapidly rising sea level moves depocenters landward. Lack of terrigenous input may concentrate hemipelagic and pelagic sediments in a thin interval that represents increasingly more time basinward. The condensed section represents the time of maximum flooding of the shelf and occurs largely within the transgressive and distal highstand systems tracts. On seismic lines it is expressed as the "*downlap surface*" (Fig. 1). Other types of condensed sections can develop independently of sea-level fluctuations on sediment-starved, current-swept, deeply subsided plateaus located in deep basins (such as the Blake Plateau during the past 20 m.y.).

SURVEY AND DRILLING DATA

The survey data used for specific site selections are discussed in each chapter. Pre-site surveys using a precision echo-sounder and seismic profiles were made on board *JOIDES Resolution*. Sonobuoys were deployed at Sites 760, 761, 762, 763, and 764. Geophysical-survey data (seismic profiles) collected during Leg 122 are presented in the "Underway Geophysics" chapter (this volume).

The seismic-profiling systems consisted of two 80-in.^{3} water guns, a 100-m-long hydrophone array designed at Scripps Institution of Oceanography, Bolt amplifiers, two band-pass filters, and two Raytheon recorders, usually recording at two different filter settings (25–250 and 25–150 Hz) and two different scales.

The 3.5- and 12-kHz bathymetric data were displayed on Precision Depth Recorder (PDR) systems. The depths were converted on the basis of an assumed 1500 m/s sound velocity. The water depth (in meters) at each site was corrected (1) for the variation in sound velocity with depth using Carter's Tables (1980), and (2) for the depth of the hull transducer (6.8 m) below sea level. In addition, depths referred to the drilling-platform level are assumed to be about 11.4 m above the water line, based on the ship's draft (Fig. 2).

Magnetic data were recorded using a Geometrics 801 proton precession magnetometer and were displayed on a strip chart recorder.

DRILLING CHARACTERISTICS

Because water circulation downhole is open, cuttings are lost onto the seafloor and cannot be examined. The only available information about sedimentary stratification in uncored or unrecovered intervals, other than that from seismic data or wireline-logging results, is from an examination of the behavior of the drill string as observed and recorded on the drilling platform. The harder a layer, the slower and more difficult it is to penetrate. A number of other factors, however, determine the rate of penetration, so it is not always possible to relate drilling time directly to the hardness of the layers. Bit weight and revolutions per minute, recorded on the drilling recorder, influence the penetration rate.

DRILLING DEFORMATION

When cores are split, many show signs of significant sediment disturbance, including the downward-concave appearance of originally horizontal bands, the haphazard mixing of lumps of different lithologies (mainly at the tops of cores), and the near-fluid state of some sediments recovered from tens to hundreds of meters below the seafloor. Core deformation probably occurs during any of several steps at which the core may experience stresses sufficient to alter its physical characteristics: cutting, retrieval (with accompanying changes in pressure and temperature), and core handling on deck.

SHIPBOARD SCIENTIFIC PROCEDURES

Numbering of Sites, Holes, Cores, and Samples

Drill sites are numbered consecutively from the first site drilled by *Glomar Challenger* in 1968. A site number refers to one or more holes drilled while the ship was positioned over one acoustic beacon. Multiple holes may be drilled at a single site by pulling the drill pipe above the seafloor (out of one hole), moving the ship some distance from the previous hole, and then drilling another hole.

For all ODP drill sites, a letter suffix distinguishes each hole drilled at the same site. For example, the first hole drilled

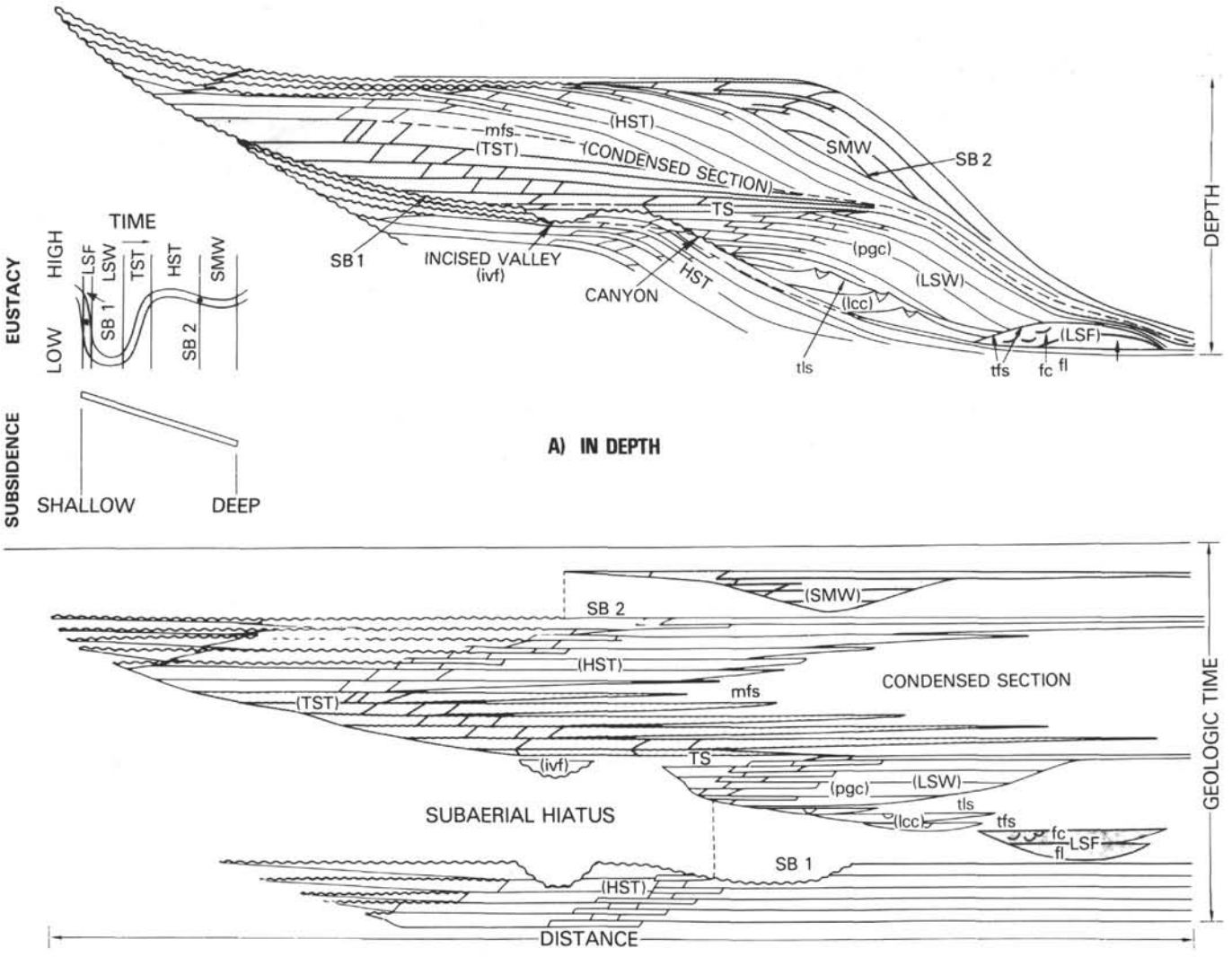

LEGEND

SURFACES

(SB) SEQUENCE BOUNDARIES
- (SB 1) = TYPE 1
- (SB 2) = TYPE 2

(DLS) DOWNLAP SURFACES
- (mfs) = maximum flooding surface
- (tfs) = top fan surface
- (tls) = top leveed channel surface

(TS) TRANSGRESSIVE SURFACE
- (First flooding surface above maximum regression)

SYSTEMS TRACTS

HST = HIGHSTAND SYSTEMS TRACT

TST = TRANSGRESSIVE SYSTEMS TRACT

LSW = LOWSTAND WEDGE SYSTEMS TRACT
- ivf = incised valley fill
- pgc = prograding complex
- lcc = leveed channel complex

LSF = LOWSTAND FAN SYSTEMS TRACT
- fc = fan channels
- fl = fan lobes

SMW = SHELF MARGIN WEDGE SYSTEMS TRACT

Figure 1. Sequence-stratigraphic concepts (from Haq et al., 1987). Depositional model showing systems tracts during the development of type 1 and type 2 sequences that occur after type 1 and type 2 unconformities, respectively. **A.** The systems tracts in relation to depth. **B.** The same features plotted against geologic time (legend below this figure explains the symbols).

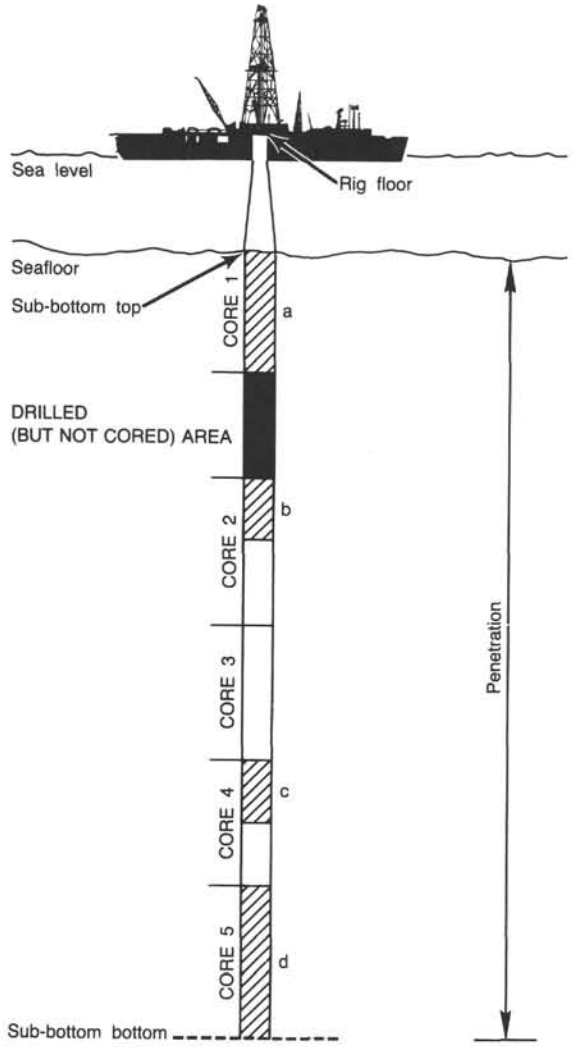

BOTTOM FELT: distance from rig floor to seafloor

TOTAL DEPTH: distance from rig floor to bottom of hole (sub-bottom bottom)

PENETRATION: distance from seafloor to bottom of hole (sub-bottom bottom)

NUMBER OF CORES: total of all cores recorded, including cores with no recovery

TOTAL LENGTH OF CORED SECTION: distance from sub-bottom top to sub-bottom bottom minus drilled (but not cored) areas in between

TOTAL CORE RECOVERED: total from adding a, b, c, and d in diagram

CORE RECOVERY (%): equals TOTAL CORE RECOVERED divided by TOTAL LENGTH OF CORED SECTION times 100

Figure 2. Diagram of terms used to discuss coring operations and core recovery.

is assigned the site number modified by the suffix A the second hole takes the site number and suffix B, etc. Note that this procedure differs slightly from that used by DSDP (Sites 1 through 624), but prevents ambiguity between site- and hole-number designations. It is important, for sampling purposes, to distinguish among holes drilled at a site, because recovered sediments or rocks from different holes usually do not come from equivalent positions in the stratigraphic column.

The cored interval is measured in meters below seafloor (mbsf). The depth interval assigned to an individual core begins with the depth below the seafloor that the coring operation began, and extends to the depth that the coring operation ended (see Fig. 2). For example, each coring interval is generally up to 9.5 m long, which is the length of a core barrel; however, coring intervals may be shorter and are not necessarily adjacent to each other, but may be separated by drilled intervals. In soft sediment, the drill string can be "washed ahead" with the core barrel in place (but not recovering sediment) by pumping water down the pipe at high pressure to wash the sediment out of the way of the bit and up the space between the drill pipe and wall of the hole. However, if thin, hard, layers are present, then it is possible to get "spotty" sampling of these resistant layers within the washed interval and thus have a cored interval greater than 9.5 m. In drilling hard rock, a center bit may replace the core barrel if it is necessary to drill without core recovery.

Cores taken from a hole are numbered sequentially from the top of the hole downward. Core numbers and their associated cored intervals (in mbsf) usually are unique in a given hole. This may not be true, however, if an interval must be cored twice, owing to caving of cuttings or other hole problems. Maximum full recovery for a single core is 9.5 m of rock or sediment contained in a plastic liner (6.6-cm internal diameter) plus about 0.2 m (without a plastic liner) in the core catcher (Fig. 3). The core catcher is a device at the

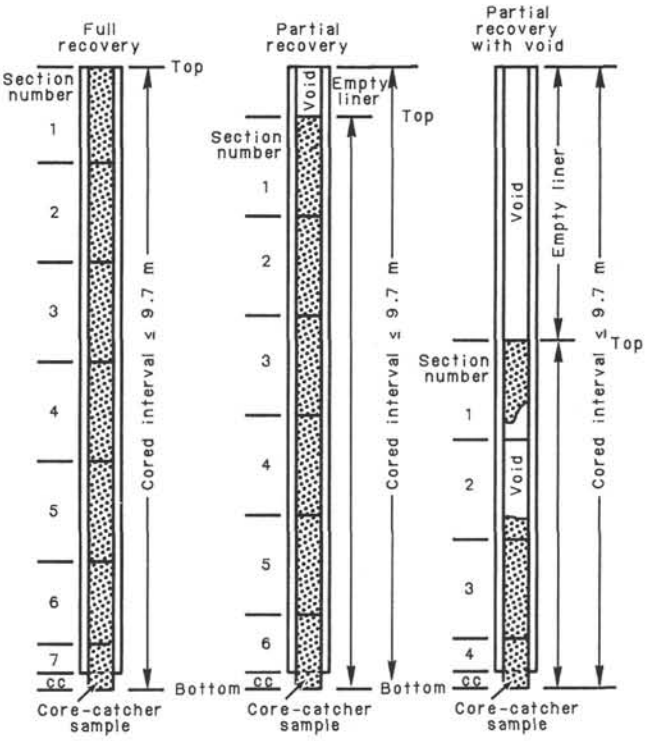

Figure 3. Diagram showing procedure used in cutting and labeling recovered core sections.

bottom of the core barrel that prevents the core from sliding out when the barrel is being retrieved from the hole. In certain situations (e.g., when coring gassy sediments that expand while being brought on deck) recovery may exceed the 9.5-m maximum.

Each recovered core is divided into 1.5-m sections that are numbered sequentially from the top (Fig. 3). When full recovery is obtained, the sections are numbered from 1 through 7 with the last section possibly being shorter than 1.5 m (rarely, an unusually long core may require more than 7 sections). When less than full recovery is obtained, there will be as many sections as needed to accommodate the length of the core recovered. For example, 4 m of core would be divided into two 1.5-m sections and one 1-m section. If cores are fragmented (recovery less than 100%), sections are numbered sequentially and intervening sections are noted as void, whether shipboard scientists believe that the fragments were contiguous *in situ* or not. In rare cases a section less than 1.5 m may be cut in order to preserve features of interest (e.g., lithological contacts).

By convention, material recovered from the core catcher is placed below the last section when the core is described, and labeled core catcher (CC); in sedimentary cores, it is treated as a separate section. The core catcher is placed at the top of the cored interval in cases where material is recovered only in the core catcher. However, information supplied by the drillers or by other sources may allow for more precise interpretation as to the correct position of core catcher material within an incompletely recovered cored interval.

A recovered basalt, gabbro, or peridotite core also is cut into 1.5-m sections that are numbered sequentially; however, each piece of rock is then assigned a number (fragments of a single piece are assigned a single number, with individual fragments being identified alphabetically). The core-catcher sample is placed at the bottom of the last section and is treated as part of the last section, rather than separately. Scientists completing visual core descriptions describe each lithologic unit, noting core and section boundaries only as physical reference points.

When, as is usually the case, the recovered core is shorter than the cored interval, the top of the core is equated with the top of the cored interval by convention, in order to achieve consistency in handling analytical data derived from the cores. Samples removed from the cores are designated by distance measured in centimeters from the top of the section to the top and bottom of each sample removed from that section. In curated hard-rock sections, sturdy plastic spacers are placed between pieces that do not fit together in order to protect them from damage in transit and in storage. Therefore, the centimeter interval noted for a hard-rock sample has no direct relationship to that sample's depth within the cored interval, but is only a physical reference to the sample's location within the curated core.

A full identification number for a sample consists of the following information: (1) leg, (2) site, (3) hole, (4) core number and type, (5) section number, (6) piece number (for hard rock), and (7) interval in centimeters measured from the top of section. For example, a sample identification of "122-759B-39R-3, 100–102 cm" would represent a sample removed from the interval between 100 and 102 cm below the top of Section 3, Core 5 (R designates that this core was taken with the rotary core barrel) of Hole 759B during Leg 122.

All ODP core and sample identifiers indicate core type. The following abbreviations are used: R = rotary barrel (RCB); H = hydraulic piston core (HPC; also referred to as APC, or advanced hydraulic piston core); P = pressure core barrel; X = extended core barrel (XCB); B = drill-bit recovery; C = center-bit recovery; I = *in-situ* water sample; S = sidewall sample; W = wash-core recovery; and M = miscellaneous material. On Leg 122, HPC, XCB, RCB, center-bit, and wash cores were recovered.

CORE HANDLING ON LEG 122

As soon as a core was retrieved on deck during Leg 122, a sample was taken from the core catcher and sent to the paleontological laboratory for an initial age assessment.

The core was then placed on the long horizontal rack, and gas samples were taken by piercing the core liner and withdrawing gas into a vacuum-tube sampler. Voids within the core were sought as sites for gas sampling. Some of the gas samples were stored for shore-based study, but others were analyzed immediately as part of the shipboard safety and pollution prevention program. Next, the core was marked into section lengths, each section was labeled, and the core was cut into 1.5-m sections. Interstitial water (IW) and organic geochemistry (OG) whole-round samples were then taken. Headspace gas samples were scraped from the ends of selected cut sections on the catwalk, and sealed in glass vials for light hydrocarbon analysis. In addition, a syringe was used to take 20-cm^3 samples for pore-fluid analyses.

Each section was sealed at the top and bottom by gluing on a color-coded plastic cap: blue to identify the top of a section, and clear for the bottom. A yellow cap was placed on section ends from which a whole-round sample had been removed. The caps were usually attached to the liner by coating the end of the liner and the inside rim of the cap with acetone, and then taping the caps to the liners.

Cores were then carried into the laboratory, where the sections were labeled once more using an engraver to mark the full designation of the section. The length of the material in each section and the core-catcher sample was measured to the nearest centimeter, and this information was logged into the shipboard core-log database program.

Cores to be measured for thermal conductivity were allowed to warm to room temperature (approximately 4–6 hours on Leg 122). During this time, the whole-round sections were run through the gamma-ray attenuation porosity evaluation (GRAPE) and *P*-wave logger devices for simultaneous estimation of bulk density and porosity, and determination of sonic velocity. After core temperatures equilibrated, thermal-conductivity measurements were made immediately before the cores were split.

Cores of relatively soft material were split lengthwise into *working* and *archive* halves. The softer cores were split with a wire or saw, depending on the degree of induration. Harder cores were split with a band saw or diamond saw. Because Leg 122 cores were split with wire from bottom to top, older material could possibly have been transported up the core on the split face of each section. Investigators should be aware that the very near-surface part of the split core could be contaminated.

The *working* half of each core was sampled for both shipboard and shore-based laboratory studies. Each extracted sample was logged in the computerized sample database program with the name of the investigator receiving the sample. Records of all removed samples are kept by the Curator at ODP headquarters. The extracted samples were sealed in plastic vials or bags and labeled. Samples were routinely taken for shipboard analysis of physical properties, percentage of calcium carbonate (coulometric analysis), and for other purposes. Many of these data are reported in the site chapters.

The *archive* half was described visually. Smear slides and shipboard grain size analyses were made from samples taken

from the *archive* half, and were supplemented by thin sections taken from the *working* half. *Archive*-half sections that showed little drilling disturbance were run through the cryogenic magnetometer. The *archive* half was then photographed with both black-and-white and color film, a whole core at a time.

Both halves of the core were then put into labeled plastic tubes, sealed, and transferred to cold-storage space aboard the drilling vessel. Leg 122 cores were left on the ship for examination by the Leg 123 scientific party. After Leg 123, the cores were transferred from the ship in refrigerated ocean freight containers to cold storage at the Gulf Coast ODP Repository, at Texas A&M University, College Station, Texas.

CORE DESCRIPTION FORMS ("BARREL SHEETS")

The core description forms (Fig. 4), or "barrel sheets," summarize the data obtained during shipboard analysis of each sediment core. "Barrel sheets" and photographs of each core are grouped in the back of the book. The following discussion explains the ODP conventions used in compiling each part of the core description forms and the exceptions to these procedures adopted by Leg 122 scientists.

Core Designation

Cores are designated using leg, site, hole, and core number and type as previously discussed (see "Numbering of Sites, Holes, Cores, and Samples" above). In addition, the cored interval is specified in terms of meters below sea level (mbsl) and meters below seafloor (mbsf). On Leg 122, these depths were based on the drill-pipe measurements (DPM), as reported by the SEDCO coring technician and the ODP operations superintendent. Note that DPM values must be corrected for the height of the rig floor dual elevator stool above sea level (11.4 m during Leg 122) to yield true water depth.

Paleontological Data

Microfossil abundance, preservation, and zone assignment, as determined by the shipboard paleontologists, appear on the core description form under the heading "Biostrat. Zone/Fossil Character." The chronostratigraphic unit, as recognized on the basis of paleontological results, is shown in the "Time-Rock Unit" column. Detailed information on the zonations and terms used to report abundance and preservation is presented in the "Biostratigraphy" section (this chapter).

Paleomagnetic, Physical-Property, and Chemical Data

Columns are provided on the core description form to record paleomagnetic results, physical-property values (density, porosity, and velocity), and chemical data (percentages of $CaCO_3$ and total organic carbon determined using the Coulometrics analyzer). Additional information on shipboard procedures for collecting these types of data appears below (see "Paleomagnetics," "Physical Properties," and "Inorganic Geochemistry" sections, this chapter).

Graphic Lithology Column

The lithological classification scheme of Mazzullo, Meyer, and Kidd (1988), accepted for shipboard use by the JOIDES Sediments and Ocean History Panel, is presented here. Sediment type is represented graphically on the core description forms using the symbols illustrated in Figure 5.

Sediment Disturbance

In some cases the coring technique, which uses a 25-cm-diameter bit having a 6-cm-diameter core opening, may result in varying degrees of disturbance of the recovered core material. This is illustrated in the "Drilling Disturbance" column on the core description form (using the symbols in Fig. 6). The following disturbance categories are recognized for soft and firm sediments:

1. Slightly disturbed: bedding contacts are slightly bent.
2. Moderately disturbed: bedding contacts have undergone extreme bowing.
3. Highly disturbed: bedding is completely disturbed, sometimes showing symmetrical diapirlike structures ("flow-in").
4. Soupy: intervals are water-saturated and have lost all aspects of original bedding.

The following categories are used to describe the degree of fracturing in hard sediments (Fig. 6):

1. Slightly fractured: core pieces are in place and have very little drilling slurry or breccia.
2. Moderately fragmented: core pieces are in place or partly displaced, but original orientation is preserved or recognizable. Drilling slurry may surround fragments.
3. Highly fragmented: pieces are from the interval cored and probably in correct stratigraphic sequence (although they may not represent the entire section), but original orientation is totally lost.
4. Drilling breccia: core pieces have completely lost their original orientation and stratigraphic position and may be completely mixed with drilling slurry.

Sedimentary Structures

In cores of soft sediment (and also in some hard sediments), distinguishing between natural structures and those created by the coring process may be extremely difficult. However, where such structures were observed, they are indicated on the "Sedimentary Structure" column of the core description forms. A key to the structural symbols used on Leg 122 is given in Figure 6.

Color

Colors of sediment are determined by comparison with the Geological Society of America Rock-Color Chart (Munsell Soil Color Charts, 1971). Colors were determined immediately after the cores were split and while they were still wet. Hard sedimentary rocks (e.g., limestones) were wetted before their color was determined.

Samples

The positions of samples taken for shipboard analysis from each core are indicated in the "Samples" column of the core description form. An asterisk (*) indicates the location of smear-slide samples and a pound sign (#) indicates the location of thin sections. The symbols IW and OG designate whole-round interstitial water and frozen organic geochemistry samples, respectively.

Although not indicated in the "Samples" column, the position of samples for routine physical-property (porosity, wet-bulk density, and velocity) and geochemical (wt% $CaCO_3$ and % organic carbon) analyses are indicated by dots in the "Physical Properties" and in "Chemistry" columns.

Shipboard paleontologists generally make age determinations on the basis of core-catcher samples, although additional samples from other parts of the core may be examined as required. Examination of such samples may lead to the recognition of zonal boundaries in the core; these are indicated in the appropriate column.

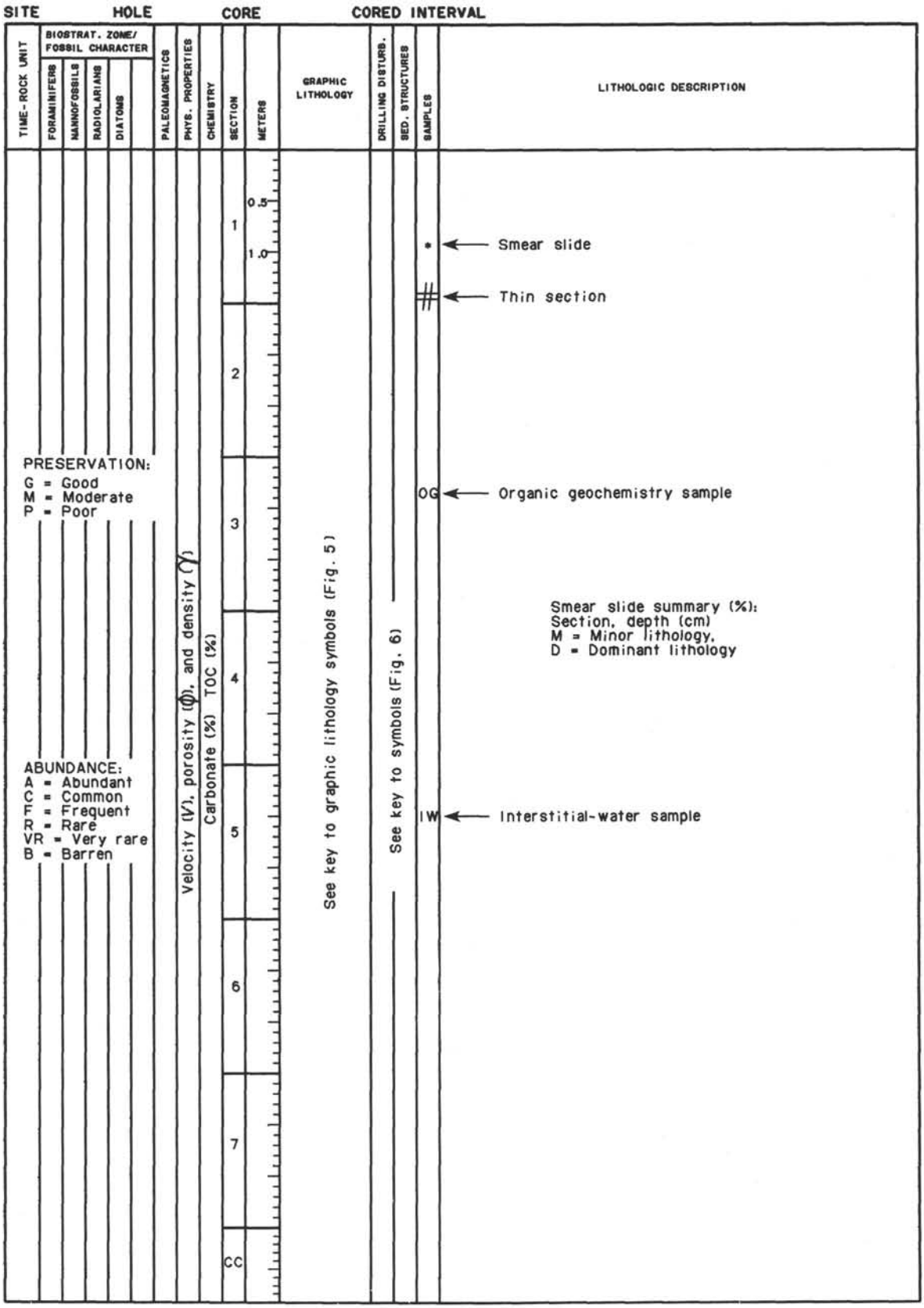

Figure 4. Core description form ("barrel sheet") used for sediments and sedimentary rocks.

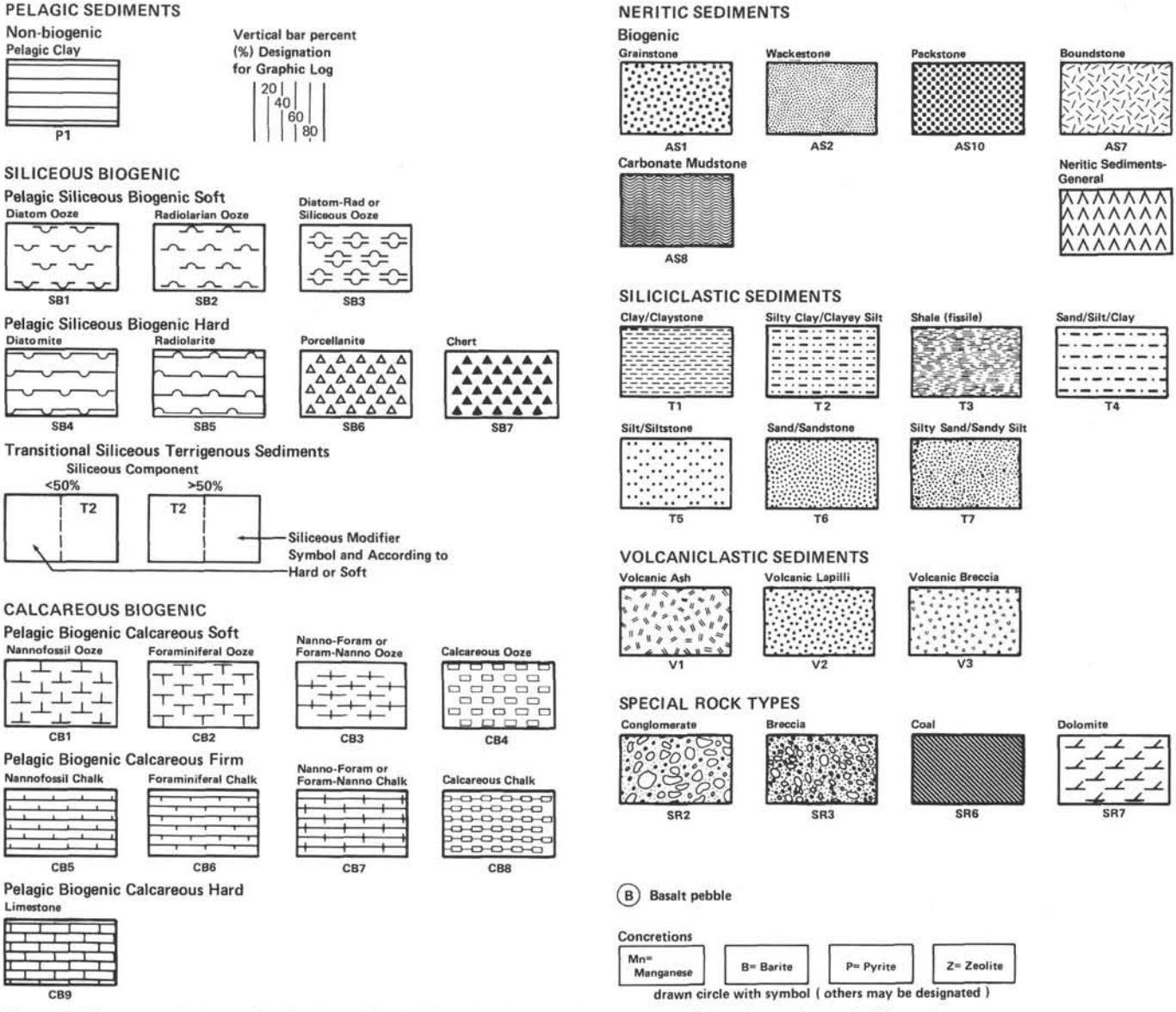

Figure 5. Key to symbols used in the "graphic lithology" column on the core description form shown in Figure 4.

Lithologic Description—Text

The lithologic description that appears on each core description form generally consists of two parts: (1) a brief summary of the major lithologies observed in a given core, followed by a description of sedimentary structures and features, and (2) a description of minor lithologies observed in the core, including data on color, occurrence in the core, and significant features.

Smear-Slide Summary

A table summarizing smear-slide and thin-section data, if available, appears on each core description form. The section and interval from which the sample was taken are noted, as well as identification as a dominant (D) or minor (M) lithology in the core. The percentage of all identified components is indicated. As explained below, these data are used to classify the recovered material.

SEDIMENT CLASSIFICATION

The new classification scheme for the Ocean Drilling Program by Mazzullo, Meyer, and Kidd (1988), partly reproduced below, was used during Leg 122. The sediment classification scheme described here defines two basic sediment types: (1) *granular* sediment and (2) *chemical* sediment.

Granular Sediments

Classes of Granular Sediments

There are four types of grains that can be found in granular sediments: *pelagic*, *neritic*, *siliciclastic*, and *volcaniclastic* grains. *Pelagic* grains are composed of the fine-grained skeletal debris of open-marine siliceous and calcareous microfauna and microflora (e.g., radiolarians, nannofossils) and associated organisms. *Neritic* grains are composed of coarse-grained calcareous skeletal debris (e.g., bioclasts, peloids), and fine-grained calcareous grains of non-pelagic origin. *Si-*

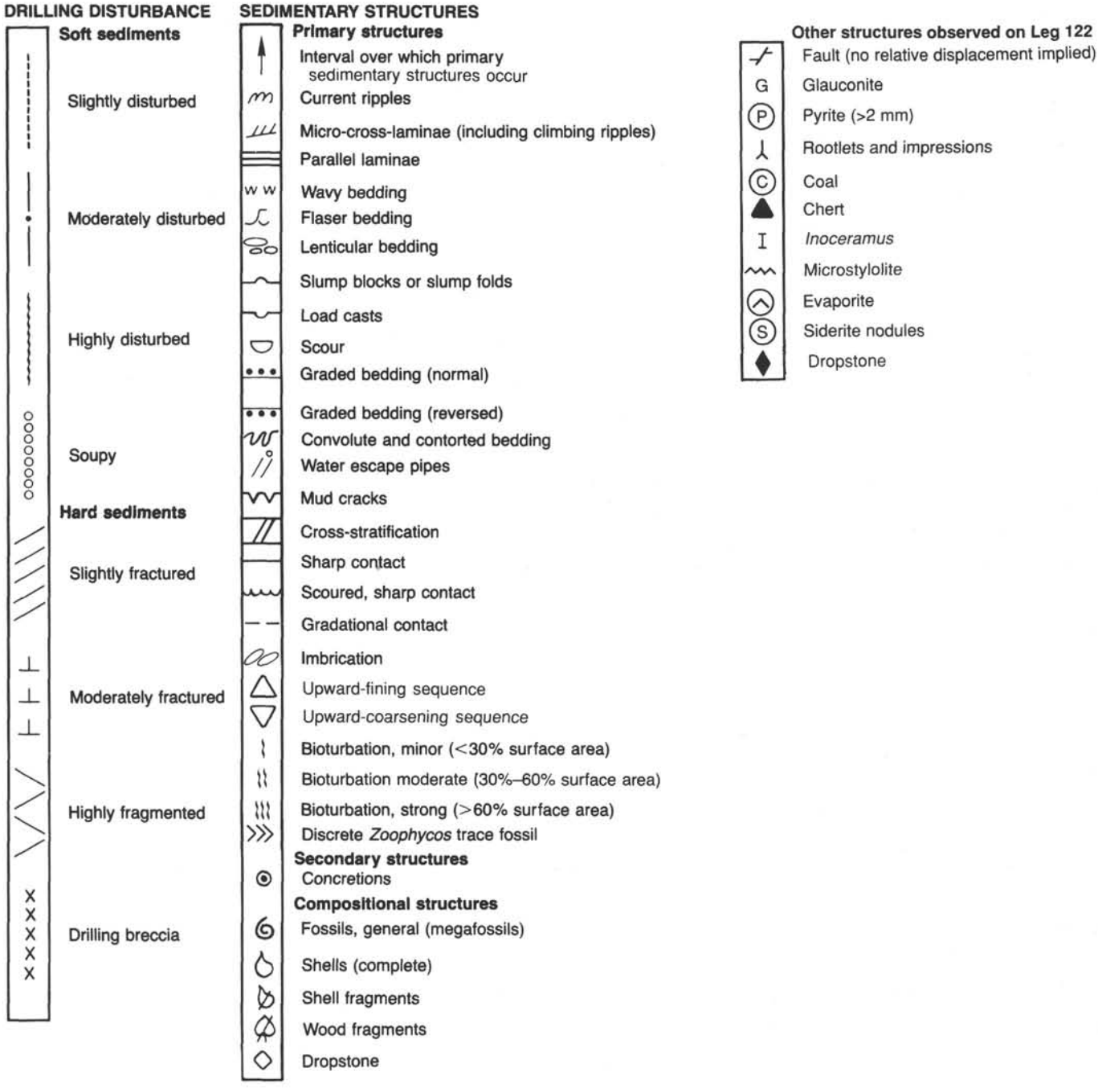

Figure 6. Symbols used for drilling disturbance and sedimentary structure on core description forms shown in Figure 4.

liciclastic grains are composed of mineral and rock fragments that were derived from plutonic, sedimentary, and metamorphic rocks. *Volcaniclastic* grains are composed of rock fragments and minerals that were derived from volcanic sources.

Variations in the relative proportions of these four grain types define five major classes of granular sediments: *pelagic*, *neritic*, *siliciclastic*, *volcaniclastic*, and *mixed sediments* (Fig. 7).

Pelagic sediments are composed of more than 60% pelagic and neritic grains and less than 40% siliciclastic and volcaniclastic grains, and contain a higher proportion of pelagic than neritic grains.

Neritic sediments are composed of more than 60% pelagic and neritic grains and less than 40% siliciclastic and volcaniclastic grains, and contain a higher proportion of neritic than pelagic grains.

Siliciclastic sediments are composed of more than 60% siliciclastic and volcaniclastic grains and less than 40% pelagic and neritic grains, and contain a higher proportion of siliciclastic than volcaniclastic grains.

Volcaniclastic sediments are composed of more than 60% siliciclastic and volcaniclastic grains and less than 40% pelagic and neritic grains, and contain a higher proportion of volcaniclastic than siliciclastic grains. This class includes epiclastic sediments (volcanic detritus produced by erosion of volcanic rocks by wind, water, and ice), pyroclastic sediments (the product of the degassing of magmas), and hydroclastic sedi-

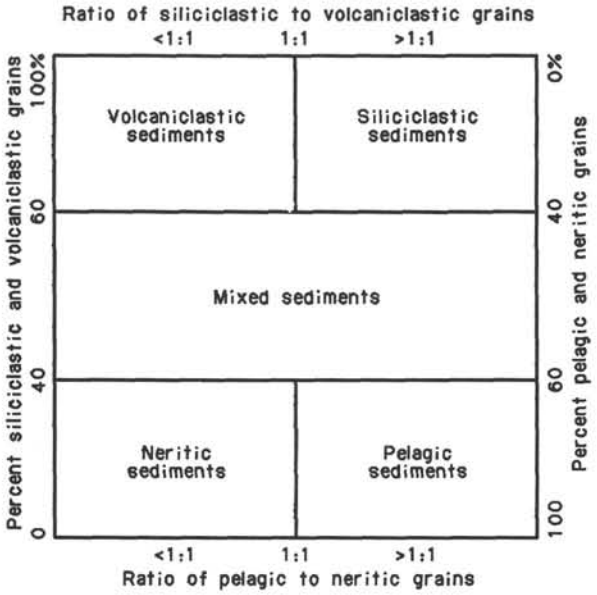

Figure 7. Diagram showing classes of granular sediments.

ments (the products of the granulation of volcanic glass by steam explosions). Lastly, mixed sediments are composed of 40%–60% siliciclastic and volcaniclastic grains, and 40%–60% pelagic and neritic grains.

Classification of Granular Sediment

A granular sediment can be classified by designating a principal name and major and minor modifiers. The principal name of a granular sediment defines its granular-sediment class; the major and minor modifiers describe the texture, composition, fabric and/or roundness of the grains themselves (Table 1).

Principal Names

Each granular-sediment class has a unique set of principal names: for pelagic sediment, the principal name describes the composition and degree of consolidation using the following terms: (1) *ooze:* unconsolidated calcareous and/or siliceous pelagic sediments; (2) *chalk:* firm pelagic sediment composed predominantly of calcareous pelagic grains; (3) *limestone:* hard pelagic sediment composed predominantly of calcareous pelagic grains; (4) *radiolarite*, *diatomite*, and *spiculite:* firm pelagic sediment composed predominantly of siliceous radiolarians, diatoms, and sponge spicules, respectively; and (5) *chert:* hard pelagic sediment composed predominantly of siliceous pelagic grains.

For neritic sediment, the principal name describes the texture and fabric, using the following terms (from Dunham, 1962): (1) *boundstone:* components organically bound during deposition; (2) *grainstone:* grain-supported fabric, no mud (during Leg 122, sediment with grains ≤2 mm was called *grainstone;* the presence of large grains was noted in the core descriptions and, where important, sediment with grains >2 mm is called *rudstone*); (3) *packstone:* grain-supported fabric, with intergranular mud, grains ≤2 mm; (4) *wackestone:* mud-supported fabric, with >10% grains (during Leg 122, sediment with grains ≤2 mm was called *wackestone;* the presence of large grains was noted in the core descriptions and, where important, sediment with grains >2 mm is called *floatstone*); (5) *calcareous mudstone:* mud-supported fabric, with less than 10% grains.

For siliciclastic sediment, the principal name describes the texture, and is assigned according to the following guidelines:

1. The Udden-Wentworth grain-size scale (Wentworth, 1922; Table 2) defines the grain-size ranges and the names of the textural groups (*gravel*, *sand*, *silt* and *clay*) and sub-groups (*fine sand*, *coarse silt*, etc.) that are used as the principal names of siliciclastic sediment.
2. When two or more textural groups or sub-groups are present in a siliciclastic sediment, they are listed as principal names in order of increasing abundance (Fig. 8; Shepard, 1954).
3. The suffix *-stone* is affixed to the principal names *sand*, *silt*, and *clay* when the sediment is lithified; *shale* is used as a principal name for a lithified and fissile siltstone or claystone. The term *mudstone* is used for indurated, non-fissile, sandy and silty, fine-grained, siliciclastic sediment, if induration, etc., precludes grain size analysis. *Conglomerate* and *breccia* are used as principal names of gravels with well-rounded and angular clasts, respectively.

For volcaniclastic sediment, the principal name describes the texture. The names and ranges of three textural groups (from Fisher and Schmincke, 1984) are as follows: (1) *volcanic breccia:* pyroclasts >64 mm in diameter; (2) *volcanic lapilli:* pyroclasts between 2 and 64 mm in diameter (3) *volcanic ash:* pyroclasts <2 mm in diameter. When lithified, the name *tuff* is used; (4) clastic sediments of volcanic provenance are described in the same fashion as siliciclastic sediments, noting the dominant composition of volcanic grains.

For mixed sediment, the principal name describes the degree of consolidation, using the terms *mixed sediments* or *mixed sedimentary rocks*.

Major and Minor Modifiers

The principal name of a granular-sediment class is preceded by major modifiers and followed by minor modifiers (preceded by the suffix "with") that describe the lithology of the granular sediment in greater detail (Table 1).

The most common uses of major and minor modifiers are to describe the composition and textures of grain types that are present in major (>25%) and minor (10%–25%) proportions. In addition, major modifiers can be used to describe grain fabric, grain shape, and sediment color. The nomenclature for the major and minor modifiers is outlined as follows.

The composition of pelagic grains can be described with the major and minor modifiers *diatom*(-aceous), *radiolarian*, *spicules*(-ar), *siliceous*, *nannofossil*, *foraminifer*(-al), and *calcareous*. The terms *siliceous* and *calcareous* are used generally to describe sediments that are composed of siliceous or calcareous pelagic grains of uncertain or, in some instances, mixed origins.

The composition of neritic grains can be described with the following major and minor modifiers: (1) *ooid* (or *oolite*): spherical or elliptical non-skeletal particles <2 mm in diameter, having a central nucleus surrounded by a rim with concentric or radial fabric; (2) *bioclast* (or *bioclastite*): fragment of skeletal remains (specific names such as molluscan or algal can also be used); (3) *pellet* (-al): fecal particles from deposit-feeding organisms; (4) *intraclast:* reworked carbonate-rock fragment or rip-up clast; (5) *pisolite:* spherical or ellipsoidal non-skeletal particle, commonly >2 mm in diameter, with or without a central nucleus but displaying multiple concentric layers of carbonate; (6) *peloid* (*pel*): micritized carbonate particle of unknown origin; and (7) *calcareous*,

Table 1. Outline of granular-sediment classification scheme.

Sediment class	Major modifiers	Principal names	Minor modifiers
Pelagic sediment	Composition of pelagic and neritic grains present in major amounts Texture of clastic grains present in major amounts	Ooze Chalk Limestone Radiolarite Diatomite Spiculite Chert	Composition of pelagic and neritic grains present in minor amounts Texture of clastic grains present in minor amounts
Neritic sediment	Composition of neritic and pelagic grains present in major amounts Texture of clastic grains present in major amounts	Boundstone Grainstone Packstone Wackestone Mudstone Floatstone Rudstone	Composition of neritic and pelagic grains present in minor amounts Texture of clastic grains present in minor amounts
Siliciclastic sediment	Composition of all grains present in major amounts Grain fabric (gravels only) Grain shape (optional) Sedment color (optional)	Gravel Sand Silt Clay	Composition of all grains present in minor amounts Texture and composition of siliciclastic grains present as matrix (for course-grained clastic sediments)
Volcaniclastic sediment	Composition of all volcaniclasts present in major amounts Composition of all pelagic and neritic grains present in major amounts Texture of siliciclastic grains present in major amounts	Breccia Lapilli Ash/tuff	Composition of all volcaniclasts present in minor amounts Composition of all neritic and pelagic grains present in minor amounts Texture of siliciclastic grains present in minor amounts
Mixed sediments	Composition of neritic and pelagic grains present in major amounts Texture of clastic grains present in major amounts	Mixed sediments	Composition of neritic and pelagic grains present in minor amounts Texture of clastic grains present in minor amounts

dolomitic, aragonitic, and *sideritic:* these modifiers should be used to describe the composition of carbonate mud or mudstone (micrite) of non-pelagic origins.

The texture of siliciclastic grains is described by the major and minor modifiers *gravel, sand, silt*, and *clay*. The composition of siliciclastic grains can be described by: (1) mineralogy: using modifiers such as "quartz," "feldspar," "glauconite," "mica," "kaolinite," "zeolitic," "lithic" (for rock fragments), "calcareous," "gypsiferous," or "sapropelic" (for detrital clasts of calcium carbonate, gypsum, and organic matter, respectively); and (2) provenance: the source of rock fragments (particularly in gravels, conglomerates, and breccias) can be described by modifiers such as volcanic, sed-lithic, meta-lithic, gneissic, basaltic, etc.

The composition of volcaniclastic grains is described by the major and minor modifiers *lithic* (rock fragments), *vitric* (glass and pumice), and *crystal* (mineral crystals), or by modifiers that describe the compositions of the liths and crystals (e.g., rhyolitic or feldspar).

The fabric of the sediment can be described by the major modifiers *grain-supported, matrix-supported,* and *imbricated.* Generally, fabric descriptors are applied only to gravels, conglomerates, and breccias, for they provide useful information on their transport history.

The shapes of grains are described by the major modifiers *rounded, sub-rounded, sub-angular,* and *angular.*

The color of sediment is determined with a standard color-comparator, such as the Munsell Chart (Munsell Soil Color Charts, 1971), and can be employed as a major modifier.

Chemical Sediments

Classes of Chemical Sediment

Chemical sediment is composed of minerals that formed by inorganic processes such as precipitation from solution or colloidal suspension, deposition of insoluble precipitates, or recrystallization of detrital evaporites, and siliceous, calcareous, or carbonaceous (plant) biogenic debris; it generally has a crystalline (i.e., non-granular) texture.

There are five classes of chemical sediments: *carbonaceous sediments, evaporites, silicates, carbonates*, and *metalliferous* sediments. Each class of chemical sediment has its own distinctive classification scheme.

Carbonaceous sediments are composed of >50% organic material (principally plant and algal remains) that has been altered by carbonization, bituminization, or putrification from its original form. The two most common varieties of carbonaceous sediments are the *coal series* and *sapropels* (sapropels were not found on Leg 122).

The *coal series* is classified according to rank. Four ranks are recognized and used as principal names: (1) *peat:* soft, earthy organic debris with recognizable plant fragments; (2)

Table 2. Udden-Wentworth grain-size scale for siliciclastic sediments (Wentworth, 1922).

mm	μm	Phi (ϕ)	Wentworth size class	
4096		−20		
1024		−12	Boulder (−8 to −12 ϕ)	
256		−8	Cobble (−6 to −8ϕ)	
64		−6		
16		−4	Pebble (−2 to −6 ϕ)	Gravel
4		−2		
3.36		−1.75		
2.83		−1.5	Granule	
2.38		−1.25		
2.00		−1.0		
1.68		−0.75	Very coarse sand	
1.41		−0.5		
1.19		−0.25		
1.00		0.0		
0.84		0.25	Coarse sand	
0.71		0.5		
0.59		0.75		
0.50	500	1.0		
0.42	420	1.25	Medium sand	
0.35	350	1.5		
0.30	300	1.75		Sand
0.25	250	2.0		
0.210	210	2.25	Fine sand	
0.177	177	2.5		
0.149	149	2.75		
0.125	125	3.0		
0.105	105	3.25	Very fine sand	
0.088	88	3.5		
0.074	74	3.75		
0.0625	63	4.0		
0.053	53	4.25	Coarse silt	
0.044	44	4.5		
0.037	37	4.75		
0.031	31	5.0	Medium silt	
0.0156	15.6	6.0	Fine silt	
0.0078	7.8	7.0	Very fine silt	
0.0039	3.9	8.0		Mud
0.0020	2.0	9.0		
0.00098	0.98	10.0	Clay	
0.00049	0.49	11.0		
0.00024	0.24	12.0		
0.00012	0.12	13.0		
0.00006	0.06	14.0		

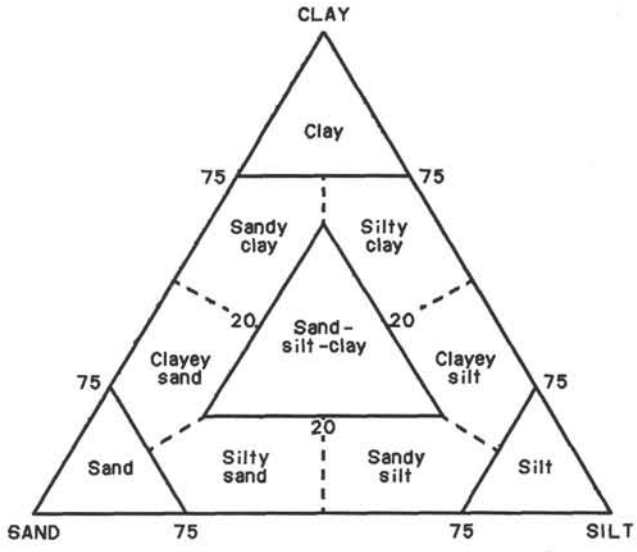

Figure 8. Ternary diagram showing principal names for siliciclastic sediments (from Shepard, 1954).

brown coal: few recognizable plant fragments, but the coal is soft, dull and brown; (3) *bituminous coal:* black and hard, contains bright layers and breaks along cleats into cuboidal fragments; and (4) *anthracite coal:* bright and lustrous, with conchoidal fractures.

The principal name of the coal series can be modified by terms that describe non-carbonaceous components such as clastic detritus (e.g., muddy peat).

Evaporites are composed of minerals produced from a saline solution that became concentrated by evaporation of the solvent. The evaporites are classified according to their mineralogy using terms such as *halite*, *gypsum*, and *anhydrite*. They may be modified by terms that describe their structure or fabric, such as massive, nodular, nodular-mosaic, and chicken wire.

Silicates and *carbonates* are defined as sedimentary rocks that are non-granular and non-biogenic in appearance and composed of silicate and carbonate minerals. Silicates and carbonate may have formed from the recrystallization of siliceous and calcareous grains, but are distinguished by the absence of clearly identifiable granular and biogenic components. They may also form as primary precipitates (e.g., dolomite or proto-dolomite) or as hydrothermal alteration products (e.g., zeolites). They are classified according to their mineralogy, using principal names such as chert (microcrystalline quartz), calcite, and dolomite. They should also be modified with terms that describe their crystalline (as opposed to granular) nature, such as crystalline, microcrystalline, massive, and amorphous.

Metalliferous sediments include a broad range of non-granular non-biogenic sedimentary rocks such as pyrite, goethite, manganese, chamosite, glauconite, and other metal-bearing minerals. They are classified according to their mineralogy.

Grain-Size Measurements

For routine assignment of sediments to textural classes, grain sizes were estimated visually from the core material, smear slides, and thin sections.

BIOSTRATIGRAPHY

Time Scales

The chronostratigraphy of Haq et al. (1987, 1988) was followed for both the Cenozoic and Mesozoic (Fig. 9).

Calcareous Nannofossils

Zonation

Zonation schemes applied in the Cenozoic included those of Gartner (1977) for the Pleistocene and Martini (1971) for the remainder of this era. Both of these zonations were successfully applied in the Indian Ocean. No Mesozoic nannofossil zonation yet developed has demonstrated worldwide applicability, and this is also very evident on the Exmouth Plateau. In the upper Cretaceous (Turonian-Maestrichtian) the zonations of Sissingh (1977) and Roth (1978) were not applicable in numerous intervals because of the absence of markers, and the different order of events observed. It is clear that a regional zonation needs to be developed from this and the other Indian Ocean legs, although this cannot be accomplished with the present data set.

For the current study we have relied largely on biohorizons. Several of these allow us to define combined zonal units

of both the Sissingh (1977) and Roth (1978) zonations as shown in Figure 10. This diagram shows the relative sequence and age of the events, but not their true stratigraphic position. Middle Cretaceous (Aptian-Turonian) zonations proved to be more successful and were compiled from Thierstein (1971, 1973). For the lower Cretaceous (Berriasian-Aptian) interval we used the zonations of Bralower (1987) and Bralower et al. (1989), which were modified from those of Thierstein (1971, 1973) and Roth (1978).

Nannofossil Relative Abundance and Preservation

For the Cenozoic and upper Cretaceous samples, wherein nannofossils compose a sizeable proportion of the total particles in a slide, the following distinctions were made in relative abundance estimates (number of specimens per fields of view): A (abundant), >10/field; C (common), 1–10/field; F (few), 1/2–10 fields; R (rare), 1/11–100 fields; V (very rare), 1/101–1000 fields. In all cases a magnification of 1250× was used to estimate relative abundance.

In the remainder of the Mesozoic, where nannofossils compose a much smaller fraction of all particles observed, a different technique was used to estimate relative abundance. In these samples, after two traverses of a smear slide at 1250× magnification, a species was listed according to number of specimens observed: A (abundant), >100; C (common), 11–100; F (few), 3–10; R (rare), 1–2.

In all samples, regardless of age, an estimate was made of the total nannofossil abundance in the following fashion. Nannofossils were listed according to the percentage of all particles for which they accounted: A (abundant), >10%; C (common), 1–10%; F (few), 0.1–1%; R (rare), <0.1%.

An estimate of preservation was made using the following terms: good (indicated by "G") preservation indicates little or no overgrowth or etching, whereas the degree of overgrowth and/or etching, where present, is indicated by moderate (M) or poor (P). In addition, a description of the degree of etching and overgrowth was made for particularly important intervals, following the guidelines of Roth and Thierstein (1972). The symbol E indicates the degree of etching, with E-1, E-2, and E-3 indicating slight, moderate, and severe etching, respectively. Similarly O-1, O-2, and O-3 indicate slight, moderate, and severe overgrowth, respectively.

Planktonic Foraminifers

Zonation

Neogene

Typical low-latitude, tropical-to-subtropical faunas dominated the Neogene assemblages. The tropical zonation scheme proposed by Banner and Blow (1965) and elaborated by Blow (1969, 1979) was applied successfully to the Exmouth Plateau, as it was to Ninetyeast Ridge (Shipboard Scientific Party, 1989).

Paleogene

The tropical zonation scheme of Blow (1969, 1979) was applied to the low-latitude faunas down to and including the upper Eocene, with application of the minor adjustments made by Berggren and Miller (1988). Middle Eocene and older Paleogene faunas were dated using the recapitulation of Berggren's (1969) zonation as given by Berggren and Miller (1988). This zonation differs from that Blow (1979), especially in the early Eocene where zones bearing the same P number in both zonations (e.g., Zone P7) show no overlap in time.

Application of the above tropical schemes offered no difficulty, although paleolatitudes of the Exmouth Plateau must have been higher than at present. This may be the result of a globally warmer climate during the Eocene and Paleocene and the cosmopolitan character of Oligocene faunas.

Mesozoic

For the Mesozoic, the zonation scheme of Caron (1985) was used down to and including the upper Albian. Some modification of this scheme was necessary around the Santonian/Campanian boundary. Below the upper Albian, planktonic foraminiferal recovery was poor and no particular scheme could be applied.

Abundance and Preservation

The abundance of a particular species in an assemblage was estimated on a visual estimate of the >63-μm size fraction. The following terms were used to report abundance: *abundant*, >20%; *common*, 10%–20%; *few*, 1%–10%; *rare*, <1%; and *barren*.

The state of preservation of planktonic foraminifers was estimated as follows: *good*, little or no evidence of overgrowth, dissolution, or abrasion; *moderate*, overgrowth, dissolution, or abrasion common but minor; and *poor*, substantial overgrowth, dissolution, or fragmentation.

Sample Preparation

Samples were prepared by soaking in hydrogen peroxide, washing through a 63μm-mesh sieve, and drying under a Fisher Infra-Radiator. Consolidated sediments were also treated ultrasonically.

Benthic Foraminifers

Zonation

The Cenozoic bathyal and abyssal calcareous benthic foraminiferal zonation of Berggren and Miller (in press) was used to date deep-water assemblages. This scheme has the advantage that it can be used in conjunction with Van Morkhoven et al. (1986) for identification of taxa. For the Mesozoic, we relied on a variety of sources of information including Dailey (1983) and Moullade (1984), both for the South Atlantic Ocean; no Indian Ocean reference is available to date. For the Triassic, Zaninetti (1976) was used.

Paleodepth Zonation

The paleodepth estimates for the Cenozoic are made on the basis of the depth ranges given by Van Morkhoven et al. (1986): neritic (0–200 m), upper bathyal (200–600 m), middle bathyal (600–1000 m), lower bathyal (1000–2000 m), and abyssal (>2000 m).

Paleobathymetric schemes for the Cretaceous are largely qualitative. Our interpretations are based on Sliter's (1977) work on DSDP Leg 36 (Upper Cretaceous) and on Moullade (1984, mid-Cretaceous); both refer to sections in the South Atlantic. At some time in the future the Indian Ocean data should be assessed independently. For the older Mesozoic shallow water deposits, sedimentological evidence and the relative abundances of morphogroups were taken into account in our environmental interpretations, as in Schott (1984).

Abundance and Preservation

The abundance of benthic foraminifers in the sediment was registered as follows (in terms of percent of the benthic fauna): *abundant*, >20%; *common*, 10%–20%; *few*, 5%–10%; and *rare*, <5%.

Preservation was noted as follows (in terms of dissolution effects): *good*, little effect; *moderate*, effects obvious but do not affect identification; and *poor*, identification difficult or impossible.

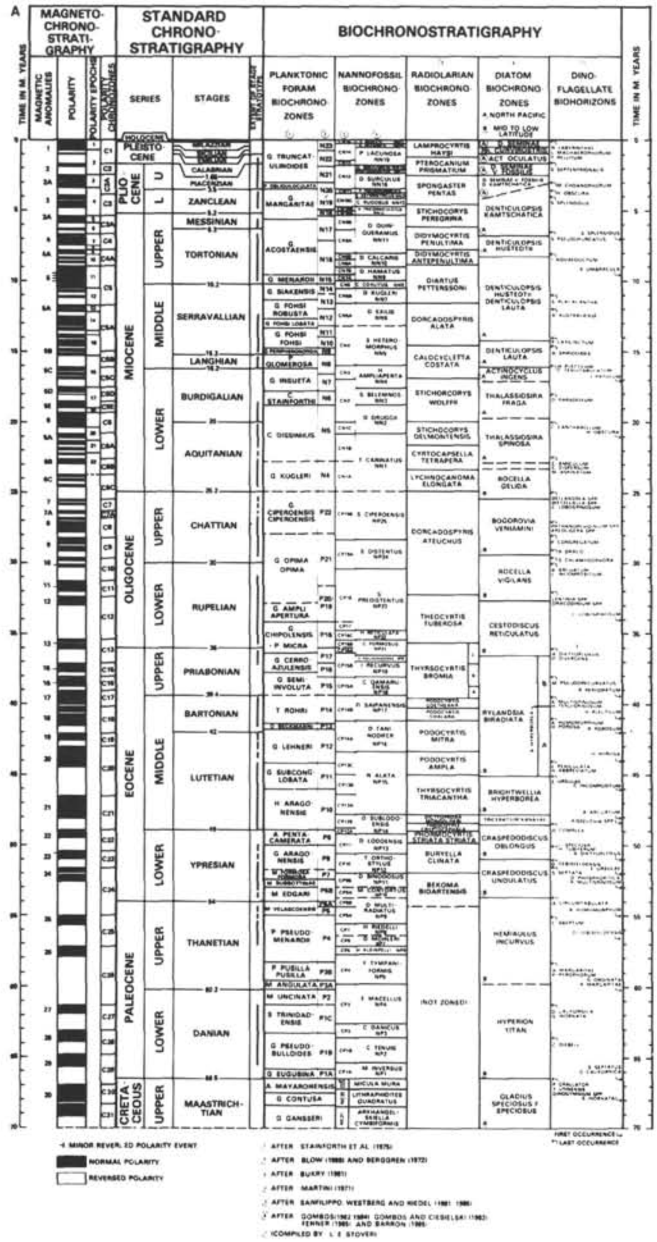

Figure 9. Chronostratigraphy of Haq et al. (1987, 1988) and correlation with magnetostratigraphy and biostratigraphy. **A.** Cenozoic **B.** Cretaceous. **C.** Jurassic. **D.** Triassic.

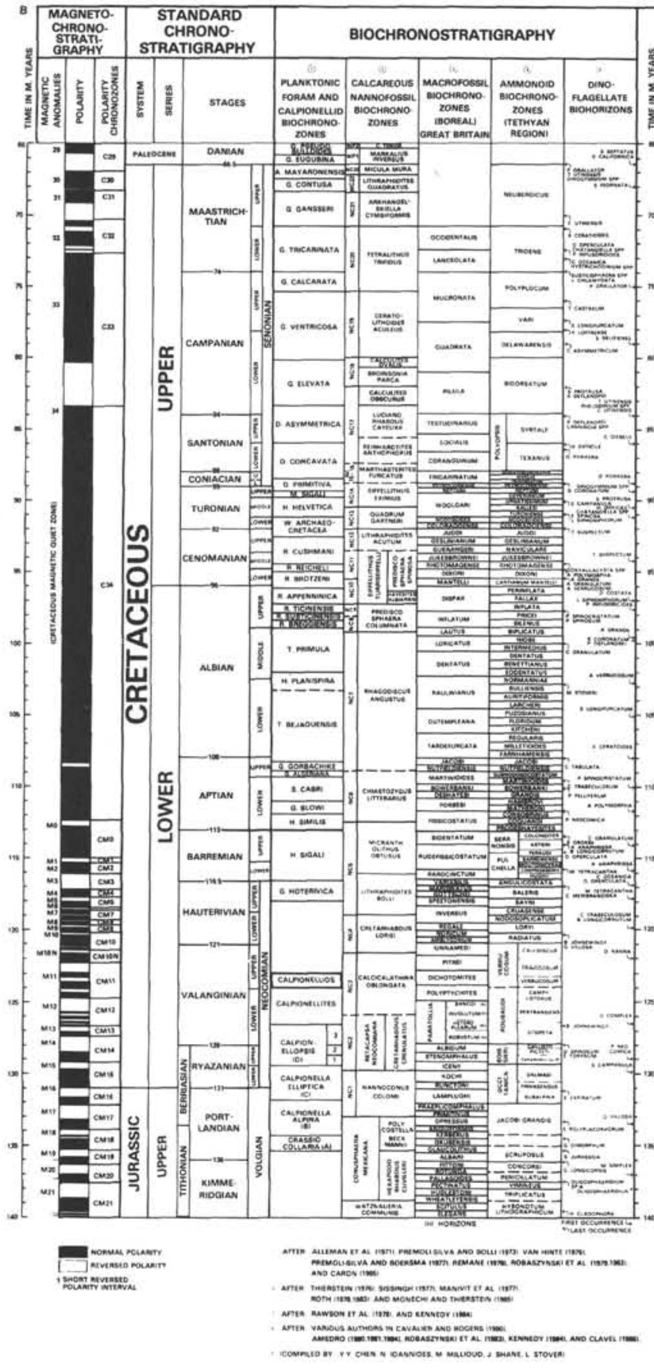

Figure 9 (continued).

Sample Preparation

The sample residues used were the same as for planktonic foraminifers.

Radiolarians

Zonation

The Leg 122 Cenozoic radiolarian faunas were assigned to biozones initially proposed by Riedel and Sanfilippo (1978), and later modified by Sanfilippo et al. (1985). No single radiolarian zonation could be used for the Mesozoic radiolarian faunas. This report uses the Cretaceous biozonation proposed by Sanfilippo and Riedel (1985) on the basis of their studies of Cretaceous material from the Deep Sea Drilling Project and Ocean Drilling Program. Supplemental faunal ranges from onshore upper Cretaceous sections were taken from Pessagno (1976), Taketani (1982), and Yamasaki (1987). Faunal data from other lower Cretaceous sections were taken from Schaaf (1981, 1984), Baumgartner (1984), and Aita (1987).

Abundance and Preservation

Radiolarian abundance data discussed in the biostratigraphy sections of the site chapters are based on slides of sieved acid residues. Consequently, observations may differ markedly from the lithologic descriptions, which are made on the basis of smear-slide data. Our abundance estimates are completely qualitative, and are determined on the visual approx-

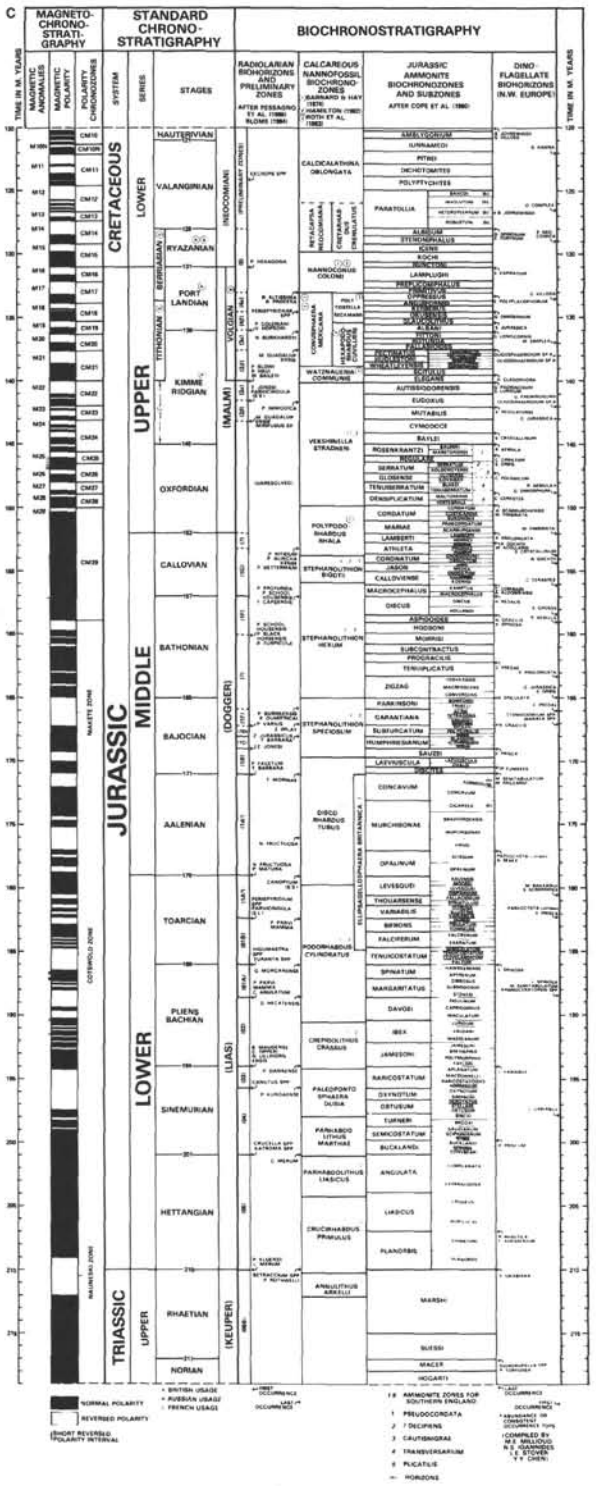

Figure 9 (continued).

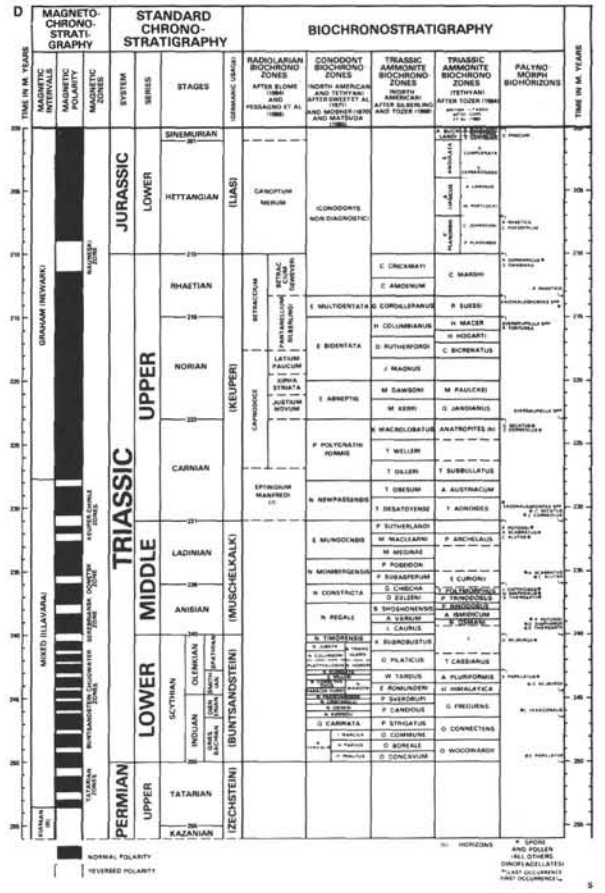

Figure 9 (continued).

imation of the total number of specimens observed per microscope traverse. We suggest that our abundance terms have the following range of absolute frequency (specimens per traverse): *abundant*, >200; *common*, 100–200; *few*, 50–100; and *trace*, <50.

Radiolarian preservation in Leg 122 sediments ranged from poor to excellent. Degraded preservation was largely a result of dissolution effects. Preservation is defined as follows: *excellent*, nearly all the specimens observed are complete, with spines intact and no overgrowths; *good*, a majority of specimens are complete, with most spines intact and little or no overgrowths; *moderate*, a substantial portion of the specimens are broken, and some degree of overgrowth or etching exists; *poor*, specimens are mostly broken and fragmentary, and show substantial overgrowth.

Sample Preparation

Most radiolarians could be studied after the sample was boiled in hydrogen peroxide for approximately 5 min, sieved, and treated with hydrochloric acid (and, if necessary, 5 s of ultrasound). If the sediment proved to be difficult to disaggregate, this procedure was repeated several times. For Cenozoic faunas, a small part of the residue (in water) was placed on a heated glass slide, and a few drops of xylene added to remove air from the individual tests. This was followed by a drop of Piccolyte or Canada basalm and a cover slip. The skeletons of most Mesozoic radiolarians are quartz and cannot be examined using standard transmitted-light techniques. These residues were simply sieved, dried, and examined using reflected-light methods.

Palynomorphs

Palynomorphs (dinoflagellate cysts, spores, pollen, organic coatings of foraminifers, and cuticles) from core-catcher samples and selected sediment samples were examined microscopically during Leg 122. Only the core-catcher samples were processed on the ship, using a quick preparation technique.

Sample Preparation

The samples were treated with 10% HCl and sieved through 20-μm meshes to remove fine sand and clay. After

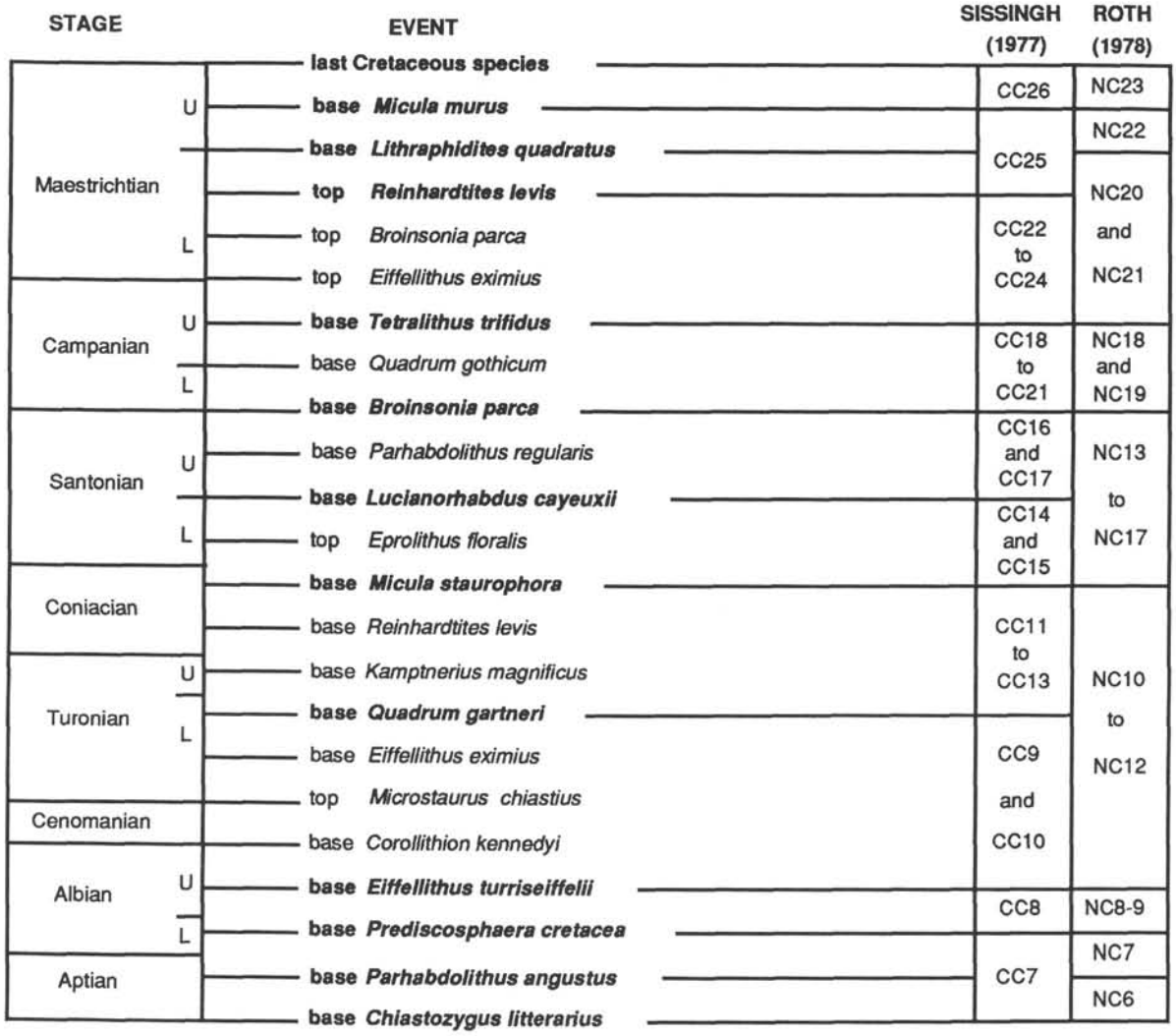

Figure 10. Upper Cretaceous calcareous nannofossil zonation scheme applied in the Exmouth Plateau sites, and correlation with previous zonations of Sissingh (1977) and Roth (1978). Events in bold indicate zonal boundaries.

sieving, the residue was put in a watch glass. Rotation of the watch glass concentrated the palynomorphs in the middle-to-upper part of the solution, where they could be extracted with a pipette.

For the normal preparation technique the sample is treated with 35% HCl and 45% HF, then sieved through 10-μm meshes to remove carbonates, silicates, and diffuse organic material.

Palynomorph Abundance and Preservation

The abundance of palynomorph species in the assemblage was registered as follows: *abundant*, >20%; *common*, 10%–20%; *few*, 2%–9%; and *rare*, 1% or less.

This scale was also used to estimate the abundance of palynomorph groups (i.e., dinoflagellate cysts, spores/pollen, cuticles/wood, and the organic coating of foraminifers).

The preservation of palynomorphs were evaluated using the following criteria:

G = good (>75% undamaged specimens, i.e., not oxidized, broken or folded).

M = moderate (25%–75% undamaged specimens).

P = poor (<25% undamaged specimens).

Palynomorph Zonation

The palynomorph zonation used for Leg 122 is the comprehensive Mesozoic zonation derived in Australia by Helby et al. (1987). The zones are range zones, concurrent range zones, and well-defined acme zones (Hedberg, 1976). Cycles of variation in spore-pollen/cuticles and dinoflagellate/spore-pollen ratios are also used to make stratigraphic interpretations.

PALEOMAGNETICS

Sampling

In general, samples were taken from the working half of the split cores as follows: 1 per section from Cenozoic and upper Cretaceous sediments, and 2–3 per section from lower Cretaceous, Jurassic, and Triassic sediments. Soft sediments were sampled by pushing 7-cm^3 plastic cubes into the section. Harder sediments were sampled by drilling 11-cm^3 minicores (2.5-cm diameter, 2.2-cm length).

Magnetic Experiments

The magnetic experiments made in the shipboard paleomagnetic laboratory can be subdivided into three complementary parts:

1. The natural remanent magnetization (NRM) and remanence after 9-mT demagnetization of all archive core halves was measured with the 2G-Enterprises 760R cryogenic magnetometer at 10- or 5-cm intervals. This gave the values of declination, inclination, and magnetization intensity for the measured intervals. The noise level of the cryogenic magnetometer was 0.1 mA/m (several orders of magnitude higher than that of similar shore-based cryogenic magnetometers), and was caused by the rolling movement of the ship. Despite the relatively high noise level, the volume of material represented by the archive half was such that all the material recovered was easily measurable. Calibration specimens brought from the University of California, Santa Cruz (UCSC), Paleomagnetics Laboratory demonstrated excellent cross-laboratory agreement.

While making measurements, results were monitored for missed jumps; sections were remeasured whenever such data anomalies were observed. The bandfilter of the SQUID (superconducting quantum interference detector) electronics was kept in a 10-Hz position. In general, this procedure is probably very effective for determining the magnetostratigraphy of young sediments (Quaternary and Late Cenozoic age). A viscous remanent magnetization (VRM) of the earth's present field direction was a common overprint of the older sediments' remanent magnetization; the 9-mT AF demagnetization was insufficient to remove this overprint. This treatment does not remove secondary chemical remanent magnetization (CRM) components due to goethite or pigmentary hematite (Lowrie and Heller, 1982; Channell et al., 1982). All of these secondary components (VRM and CRM) must be removed by alternating field treatment at high fields, or by thermal treatment to at least 300°–350°C for a VRM component (Biquand and Prévot, 1970) or higher temperature for a CRM. Such treatment is not possible with the core halves; thus, discrete samples must be used to study the direction of the primary component of magnetization of most Leg 122 Mesozoic sediments.

2. Progressive demagnetization of pilot samples was conducted in alternating-current (AC) fields up to 20 mT. Pilot sets of discrete samples (obtained from the working half of the core) representing each sedimentological unit were either measured with the cryogenic magnetometer (in a discrete-sample mode) or with the Molspin magnetometer. Pilot samples with weak NRM intensity were thermally demagnetized with the Schonstedt TSD-1 demagnetizer because this technique is more effective (although time-consuming), and because the Schonstedt AF-demagnetizer was suspected to cause an anhysteretic remanent magnetization (ARM) above 15–20 mT.

Thermal demagnetization could not be undertaken at very high temperatures because of the probable buildup of viscous magnetic components in marine sediments. Complete analysis will be undertaken on shore, especially mixed cleaning (thermal and AF demagnetization), which is very effective for removing secondary components in Mesozoic sediments (Galbrun et al., 1988).

3. Low-field magnetic-susceptibility measurements using the Bartington whole-core sensor were made at 5–20-cm intervals (however, whole-core measurements were not performed during the first three weeks of the cruise (Sites 759–761) because of the lack of regulated power on board the ship). Magnetic susceptibility provides an indication of downhole variations in the concentration of magnetic material.

SEDIMENTATION RATES

To estimate sedimentation rates, the time scale of Haq et al. (1987) was used. The methodology described below has been applied at all Leg 122 sites. For both Cenozoic and Mesozoic sedimentary sequences, ages were determined on the basis of calcareous nannofossil stratigraphy. The depths correspond to nannofossil zonal boundaries as outlined in the biostratigraphy section of each site chapter. The depth calculated for a zonal boundary is that between the two sections if samples were examined from every section (as for the Cenozoic); if samples were observed in alternate sections (as for the Mesozoic), the depth estimate is at the base of the lowest section in which the overlying zone was observed.

Errors involved in this analysis are considerable and are also quite difficult to estimate quantitatively. The major errors are associated with biostratigraphy and its calibration with chronostratigraphic units, the calibration of the time scale with radiometric ages, and the calculation of sub-bottom depths of core-catcher samples in intervals of poor recovery. However, for this analysis we do not consider all of these problems and use a standard error for both age and depth. For age, the error bar illustrated in the plots is the mean zonal duration for the interval (approximately 2 m.y. for the Cenozoic and 4 m.y. for the Mesozoic). This error takes into consideration some analytical errors associated with radiometric ages used to calibrate the time scale. The 2-m.y. error is probably too high for the Neogene, but quite accurate for the Paleogene. A 4-m.y. error is probably an underestimate for much of the lower Cretaceous.

The depth error is calculated from the stratigraphic gap between samples, which is 1.5 m for the Cenozoic and 3.0 m for the Mesozoic. Biostratigraphic errors are very difficult to estimate quantitatively and have therefore been neglected in this analysis. These are particularly high in the lower Cretaceous at Sites 762 and 763 as it was difficult to assign standard zonal units to the recovered section. In this part of the section, therefore, the applied errors are grossly underestimated.

ORGANIC GEOCHEMISTRY

The organic geochemistry program for Leg 122 included: (1) measurement of inorganic carbon concentrations, (2) determination of total organic carbon concentrations and characterization of organic matter by Rock-Eval pyrolysis, (3) analyses of hydrocarbon gases, and (4) analyses of petroleum-range hydrocarbons. Laboratory and analytical procedures are outlined here. The detailed procedures are described by Emeis and Kvenvolden (1986).

Inorganic Carbon

Percent carbonate carbon and organic carbon analyses were carried out on freeze-dried bulk samples utilizing Coulometrics 5010 coulometers coupled with the 5030 carbonate carbon analyzers. Measurements were made on headspace gas samples taken near organic geochemistry and interstitial water samples, as well as on samples used for physical-properties measurements and XRF analysis. The wt% carbonate carbon was determined by reacting 20–50 mg of ground sample in a 2N HCl solution. The quantity of liberated CO_2 was measured by titration in a monoethanolamine solution with a colorimetric indicator. The change of transmittance was monitored by a photodetection cell.

Rock-Eval and Organic Carbon

The bulk geochemical character of sedimentary organic matter was determined utilizing Rock-Eval pyrolysis techniques outlined by Espitalié et al. (1977) and Espitalié et al. (1985). The following parameters were measured during the programmed pyrolysis (300°–600°C) of 100-mg ground bulk samples: (1) the amount of "free" hydrocarbons released at 300°C (S_1), (2) the amount of hydrocarbons released (mainly as result of the cracking of kerogen) during heating to 600°C (S_2),

(3) total CO_2 released from organic matter during pyrolysis to 390°C (S_3), (4) the temperature of maximum hydrocarbon release during pyrolysis (T_{max}), and (5) the total amount of CO_2 generated during oxidation at 600°C. From these values hydrogen, oxygen, and productivity indices and total organic carbon concentrations were calculated. The hydrogen index represents the ratio of pyrolyzable organic matter or "hydrocarbons" (S_2) to total organic carbon (mg HC/g TOC). The oxygen index represents the ratio of carbon dioxide released (S_3) to total organic carbon (mg CO_2/g TOC). The production index (PI) is defined as the ratio $S_1/(S_1 + S_2)$.

Hydrocarbon Gases

For safety considerations, concentrations of C_1 (methane) and C_2 (ethane) hydrocarbon gases were monitored at 30-m intervals or whenever gas pockets were encountered. Gases were extracted using either a headspace-sampling technique for bulk sediments (Kvenvolden and Bernard, 1983; Kvenvolden and McDonald, 1985), or a vacutainer for sampling gas pockets directly through the core liner. The headspace analyses were performed by placing 5-cm^3 samples in glass containers (sealed with a septum and metal crimp) and heating them to 70°C. All gas samples were analyzed with a Carle AGC 1000/Model 211. Samples that were determined to contain notable quantities of low molecular weight hydrocarbons were also analyzed with a Hewlett Packard 5890 gas chromatograph.

Petroleum-Range Hydrocarbons

Analysis of C_{15+} hydrocarbons was done on a small number of samples of core material and potential shipboard contaminants. The procedure consisted of: (1) extraction of samples with either hexane or dichloromethane, (2) isolation of the hydrocarbon fraction of the extract by solvent chromatography on silica gel columns, and (3) injection of this fraction into a capillary-column-equipped Hewlett Packard 5890 FID gas chromatograph.

INORGANIC GEOCHEMISTRY

Interstitial Water

Shipboard interstitial water analyses were performed during Leg 122 on 5–10-cm whole-round samples from every third core (sample spacing = approximately 30 m) if sufficient material was available. At selected sites, every core in the upper 100 m of the hole was sampled; below 100 mbsf, every third core was sampled. The routine analyses included pH, alkalinity, salinity, chloride, sulfate, calcium, magnesium, and silica. *In-situ* pore water samples were also obtained. Samples were squeezed using a stainless steel press at room temperature (Manheim and Sayles, 1974) and were filtered. Alkalinity, pH, and salinity were determined immediately after filtration; samples were then refrigerated and titrations and instrumental analyses carried out within a few days of sample collection.

All shipboard chemical analyses of interstitial waters were performed with standard ODP techniques. Potentiometric alkalinity titrations and pH measurements were carried out using a Metrohm autotitrator and a Brinkman combination pH electrode (Gieskes, 1974). Total dissolved solids (salinity) were determined using a Goldberg optical refractometer. Calcium, magnesium, and chloride concentrations were determined titrimetrically as described by Gieskes (1974) and modified by Gieskes and Peretsman (1986). Sulfate was determined using a Dionex ion chromatograph (Gieskes and Peretsman, 1986). Silica was determined spectrophotometrically using the silico-molybdate method with a Bausch and Lomb Spectronic 1001 (Gieskes and Peretsman, 1986). International Association of Physical Sciences Organizations (IAPSO) standard seawater was used to standardize all shipboard analyses.

X-ray diffraction (XRD) studies were carried out on the squeeze cakes from the pore-water analyses and on other solid-phase samples of interest. A Philips system consisting of a model PW 1729 X-ray generator and APD 3720 automated powder diffraction data acquisition module equipped with a monochromator and scintillation detector was used for all XRD studies. Carbonate-rich samples in which secondary minerals were of particular interest were usually treated with a pH 5 buffer of sodium acetate/acetic acid in order to remove calcium (and magnesium) carbonate prior to obtaining diffractograms. Clay-size fractions (<2 μm) were isolated by centrifugation prior to XRD analyses and run both as oriented and standard powder mounts. XRD parameters and operating conditions were: CuKα X-radiation; generator settings = 40 kV, 35 mA; step size = 0.02° 2Θ; count time = 1.0 s; angle range = 2°–70° 2Θ.

PHYSICAL PROPERTIES

The physical properties determined on board ship were compressional velocity, velocity anisotropy, bulk density, grain density, porosity, water content, thermal conductivity, formation factor, and undrained shear strength. A summary of the methods employed during Leg 122 follows.

The Gamma-Ray Attenuation Porosity Evaluator (GRAPE), described by Boyce (1976), was used to make a continuous measurement of wet-bulk density in APC cores only. Aluminum and water standards were used to calibrate the equipment at each site. Sections of cores were mounted vertically in a rack, and the gamma-ray source and sensor were moved down the length of the core. The attenuation of the gamma rays passing through the liner and core was determined every 2 s (approximately every 1 cm) and the bulk density was calculated from the attenuation values.

The *P*-Wave Logger (PWL) is mounted on the same frame as the GRAPE, so both are run simultaneously. Two 500-kHz compressional wave transducers were moved down the length of the core, and measurements were taken every 2 s (approximately every 1 cm) perpendicular to the core axis. Water was applied to the core liner to improve acoustic contact.

After GRAPE and PWL analysis, the cores were allowed to equilibrate to room temperature for three or more hours before thermal conductivity was measured. The thermal conductivity techniques used here are described by Von Herzen and Maxwell (1959) and Vacquier (1985). Needle probes connected to a Thermcon-85 unit (interfaced with a PRO-350 computer) were inserted into the sediment through holes drilled into the liner, and the thermal drift was monitored. An additional probe was inserted into a reference material. After the temperature stabilized the probes were heated, and the coefficient of thermal conductivity was calculated as a function of the change in resistance in the probe about every 12 s over a 6-min interval.

For sediment too stiff to allow the insertion of the probe, holes were drilled into the sediment with a long, thin, drill bit. For well-lithified sediment, thermal conductivity was measured on samples from split cores with the use of a needle probe partially embedded in a slab of insulating material. The sample was placed on the slab, and both slab and sample were immersed in a salt-water bath and allowed to reach thermal equilibrium with the water. The probe was heated, and measurements of resistance changes in the probe were made every 9 s in a 6-min interval. Good contact between the slab and sample was accomplished by polishing the surface of the

sample and using Dow Corning 111 heavy silicone lubricant between them.

Undrained shear strength (Boyce, 1977; Lee, 1984) was determined using a motorized vane apparatus with four 1.28 × 1.28-cm blades. The vane was inserted into the split section of core (perpendicular to the core axis) until the top of the blade was covered by sediment. The vane was then rotated at a rate of about 65° per minute until the sediment failed. The undrained shear strength was calculated from the peak torque obtained before failure.

Electrical resistivity of the sediments was determined in terms of the formation factor (the ratio of the resistivity of the sediment to the resistivity of the pore water). Measurements were performed parallel and perpendicular to the core axis. A four-pin electrode technique was used for these measurements, similar to the method of Manheim and Waterman (1974). Four tungsten pin electrodes (two current and two potential) spaced 1 cm apart were mounted on a piece of plexiglas, and pressed into the sediment on a split core. A Wayne-Kerr Precision Component Analyzer 6425 was used to measure the resistance of the sediments between the two potential electrodes. Measurements were taken at 1 kHz and 0.5 volts AC. The electrodes were then placed into a split core liner filled with seawater and the resistance was measured. The sediment and the water thus have identical geometrical factors needed in the calculation of resistivities. The formation factor was then calculated by dividing the resistance of the sediment by the resistance of the seawater.

Samples were measured for compressional-wave velocity adjacent to intervals for which undrained shear strength and formation factor were determined, and in the same sample interval from which index properties were acquired. Velocities were calculated from the determination of traveltime for a 500-kHz compressional wave through a measured thickness of sediment sample, using a Hamilton Frame Velocimeter and Tektronix DC 5010 counter/timer system. Travel distance was measured by using an attached variable resistor (installed during this leg) connected to a Tektronix DM 5010 digital multimeter. Soft and brittle sediment samples were measured in the core liner. Lithified samples were cut into minicores and "chunks" (with at least one pair of parallel sides) and measured both perpendicular and parallel to the core axis. The Hamilton Frame was calibrated with lucite standards at the beginning of Leg 122 and checked throughout the cruise. The variable resistor was calibrated with standard lengths of aluminium cylinders and checked occasionally for any drift.

Velocity anisotropy was calculated after horizontal and vertical velocities were measured, using the equation $(V_{ph} - V_{pv})/V_{p\text{-mean}}$, where V_{ph} is horizontal velocity (perpendicular to the core axis), V_{pv} is the vertical velocity (parallel to the core axis), and $V_{p\text{-mean}}$ is the mean velocity. Anisotropy is positive when $V_{ph} > V_{pv}$.

The index properties (wet-bulk density, grain density, porosity, and water content) were determined using the velocity samples. Samples were weighed wet using two Scientech 202 electronic balances interfaced with a PRO-350 computer; the balances compensate for the ship's motion by taking the average of 250 sample weighings. Sample volumes were then determined using a Quantachrome helium Penta-Pycnometer. Weight and volume were remeasured after the samples were freeze-dried for 12 hr. Definitions used for the index properties are (1) wet-bulk density (g/cm^3) = weight of wet sediment/volume of wet sediment; (2) water content (%) = 100 × weight of seawater/weight of wet sediment; (3) porosity (%) = 100 × volume of seawater/volume of wet sediment; (4) grain density (g/cm^3) = weight of dry sediment/volume of dry sediment. Dry-sediment weights and volumes used in the above calculations were corrected for salt content (assuming seawater salinity of 35 g/kg) by subtracting the estimated weight and volume of residual salt.

The physical properties collected for samples during Leg 122 are presented in tables and figures in each site chapter. Porosity (ϕ), bulk density (ρ), and mean velocity ($V_{p\text{-mean}}$) values are also given in the physical properties column on the barrel sheets for the cores of each site.

GEOPHYSICAL WELL LOGGING

Geophysical well logging provides continuous *in-situ* measurement of physical and chemical formation parameters, which upon interpretation yield a stratigraphic, lithologic, geophysical, and mineralogic characterization of the site. Logging data may be directly correlated with core measurements when available, or used to supplement core data where recovery is poor.

The Lamont-Doherty Borehole Research Group is contracted by ODP to provide the geophysical well logging on board the *JOIDES Resolution*. Lamont-Doherty, in turn, subcontracts Schlumberger Offshore Services to run the downhole logging tools. While the logging tools used by Schlumberger are designed for use in petroleum exploration, many have proven useful for gathering information of scientific interest. In some cases individual logging sondes have been modified to meet ODP requirements, including the reduction of tool diameter to allow insertion in the 9.7-cm (3.8-in.) drillstring bore.

The full suite of Schlumberger logging tools are combined into three tool strings for maximum efficiency. These tool combinations are the seismic stratigraphic, lithoporosity, and geochemical combinations.

The seismic stratigraphic tool string includes: (1) the long spacing sonic (LSS) or sonic digital tool (SDT), (2) dual induction (DIL) or phasor induction (DIT-E) tool, (3) gamma-ray (GR) or natural gamma spectrometry tool (NGT), and (4) caliper tool (MCD). This tool combination measures compressional wave velocity, resistivity, and hole size, and estimates the proportions of the primary radioactive elements uranium (U), potassium (K), and thorium (Th).

The lithoporosity combination includes: (1) natural gamma spectrometry (NGT), (2) lithodensity (LDT), and (3) compensated neutron (CNT-G) tools. This combination provides measurements of formation porosity and density, and determines the spectral content of naturally occurring radiation.

The geochemical combination includes natural gamma spectrometry (NGT), induced gamma-ray spectrometry (GST), and the aluminum clay tool (ACT). This tool combination measures the relative concentrations of 11 elements: silicon (Si), calcium (Ca), aluminum (Al), iron (Fe), sulphur (S), manganese (Mn), hydrogen (H), chlorine (Cl), potassium (K), thorium (Th), and uranium (U).

Two additional tools (GPIT and AMS) can be run on either the lithoporosity or geochemical tool strings. The GPIT measures vector magnetic field, hole azimuth and hole deviation. The second tool, the Auxiliary Measurement Sonde, (AMS) measures hole temperature and mud resistivity.

A brief outline of the operation of each tool used on Leg 122 follows. Further information can be obtained from the Borehole Research Group at Lamont-Doherty Geological Observatory, the ODP Wireline Logging Manual, or directly from Schlumberger.

Long Spacing Sonic Tool (LSS)

The long spacing sonic tool measures the compressional wave velocity of the formation. Two acoustic sources

spaced 61 cm (2 ft) apart are separated by 2.45 m (8 ft) from two receivers also spaced 61 cm (2 ft) apart. The configuration provides interval traveltime (measured in μs/ft) for the near and far receiver pairs. These data are processed to yield formation velocity, which combined with the formation density, can be used to generate a synthetic seismogram.

Sonic Digital Logging Tool (SDT)

The basic sonic logging tool determines the transit time of a sonic pulse through the formation; this transit time measurement is usually expressed in μs/ft. The Sonic Digital Logging Tool (SDT) is a digital version of the basic sonic tool. The addition of an 8-array receiver section to a conventional paired dual transmitter/receiver sonic tool gives the SDT the capability to record many more sonic waveforms (and their associated transit times) at a given depth. Available SDT measurements are:

0.91 m (3 ft), 1.52 m (5 ft), 2.13 m (7 ft): spaced Δt measurements + waveforms.
2.45 m (8 ft), 3.05 m (10 ft), 3.66 m (12 ft): spaced Δt measurements + waveforms.
Array waveform recording for improved shear and Stoneley wave identification.
Borehole fluid Δt measurement.

The recovery of more data allows seismic signal processing techniques to be applied in order to enhance data quality. Sonic waveform recording, as opposed to recording only the first arrival times, allows the identification of later shear and Stoneley wave arrivals.

Dual Induction Tool—Model E (DIT-E) (Phasor Induction Tool)

The Dual Induction resistivity tool provides three measurements of formation resistivity: (1) deep induction (Induction Log—Deep, or ILD); (2) medium induction (Induction Log—Medium, or ILM); (3) shallow induction (Spherically Focussed Log, or SFL).

Each measurement has a characteristic depth of investigation which depends on the formation, pore fluid, and mud resistivities. Generally the ILD has the greatest depth of investigation and is therefore considered to give the best estimate of true formation resistivity. Depths of investigation are 5, 2.5, and 0.5 m (16.4, 8.2, and 1.6 ft), respectively. Vertical resolution is 1.5 m (5 ft).

The induction measurements are measurements of formation conductivity which are converted to resistivity values for ease of presentation. The induction measurement is made using a system of transmitter/receiver coil pairs. An alternating current is produced in the transmitter coils, inducing eddy currents in the formation. The magnetic field produced by these circulating eddy currents in turn induces a voltage at the receiver coil. The magnitude of the eddy current flow, and hence the receiver voltage and current, is proportional to the formation conductivity. The DIT-E tool records both a formation response signal R (90° out of phase) and a noise signal X (180° out of phase) and thus allows processing to obtain a more accurate reading of formation conductivity.

The SFL uses a focussing configuration and constant potential electrodes, and thus obtains a shallow focussed resistivity measurement. The DIT-D is the analog version of the DIT-E. Only alternating current at 20 kHz is used in the transmitter coils.

Natural Gamma Spectroscopy Tool (Natural Gamma Tool: NGT)

A basic gamma-ray (GR) tool records the natural radioactivity of a formation using a scintillation detector. This radiation is recorded initially as counts/s and is subsequently presented on an American Petroleum Institute (API) radiation scale. The NGT allows the total gamma-ray response (SGR) of a formation to be separated into three components: the contributions due to K, U, and Th. The analysis is achieved by subdividing the entire incident gamma-ray spectrum into five discrete energy windows. The total counts recorded in each window, for a specified depth in the well, are processed at the surface to give the relative elemental abundance of K, U, and Th.

Mechanical Caliper Device (MCD)

This tool provides a basic two-dimensional caliper log of the borehole by means of a bowspring-mounted measurement system. The hole diameter (HD) log is used to detect washouts or constrictions. Borehole diameter significantly affects many of the other logging measurements, and the hole diameter is an important input to log correction routines.

Compensated Neutron Tool—Model G (CNT-G)

Neutrons (5 MeV) from an americium-beryllium (Am-Be) source collide with hydrogen (H) in the formation and lose energy. These slowed neutrons are then captured by chlorine (Cl), lithium (Li), boron (B), and gadolinium (Gd), and capture gamma rays are emitted. Thus H content (both bound and free) of the formation is the primary quantity obtained with this tool, and is expressed as thermal neutron porosity. The epithermal (intermediate energy) neutron flux is an indicator of free water only, which is expressed as epithermal neutron porosity. The difference between thermal neutron porosity and epithermal neutron porosity is thus proportional to bound water in clays in the formation. The vertical resolution of this tool is 0.25 m (0.8 ft).

Lithodensity Tool (LDT)

The cesium (^{137}Cs) source in this tool emits gamma rays which interact with the electrons in the elements in the formation by Compton scattering. This transfer of energy forms the basis of the density measurement. Formation density is extrapolated from this energy flux by assuming that the atomic weight of most rock-forming elements is approximately twice the atomic number. At low energies, gamma radiation is absorbed by the photoelectric effect. The photoelectric factor (PEF) is primarily used as a matrix lithology indicator.

Gamma Spectroscopy Tool (GST)

Thermal neutrons (14 MeV) generated by this tool interact with the formation and are captured by Ca, Cl, Si, Fe, H, and S, with the resulting emission of capture gamma rays. This gamma radiation is measured by a sodium iodide (NaI) detector and the spectrum is windowed for the energies of the individual elements. Since other elements contribute somewhat to the signal, various elemental ratios are used at sea as preliminary indicators of lithology, porosity, clay mineral content, pore-fluid salinity, and evaporite content. In postcruise processing, a linear inversion method is used to obtain the dry wt% as oxides for each of the six elements above.

Aluminum Clay Tool (ACT)

The Aluminum Clay Tool (ACT) is a modified NGT paired with a modified CNT-G carrying a californium (Cf) source (2

MeV). The radiation emitted by this source primarily activates the Al, Mn, and Ca in the formation. The modified NGT measures the induced plus background activity to determine the Al and Mn concentrations. The ACT data, combined with the GST logs, is routinely used to determine clay mineralogy and to detect the presence of hydrothermal alteration and vein-filling minerals (pers. comm., E. Pratson, 1988). New methods are being developed to characterize the spatial fluxes of elements using data from the ACT.

Telecommunications Cartridge (TCC)

The telecommunications cartridge is located at the top of each tool string; it channels the data from all the tools to the surface.

HEAT FLOW

Heat-flow measurements on Leg 122 were derived from the Uyeda downhole temperature probe (T-probe), together with measurements of thermal conductivity derived from routine physical-properties data. At least two or three temperature measurements were planned for each site in order to generate a temperature gradient. These measurements were usually restricted to the upper 150 mbsf because of the difficulty of extracting the T-probe from the sediments in more resistant and cohesive lithologies.

The technique for temperature measurement (Erickson, 1984) consists of securing a thermistor probe to the bottom of the core barrel, lowering the core barrel to the base of the hole on the wireline, latching the barrel into the bottom hole assembly, and lowering the drill string to the bottom of the hole using the weight of the bottom-hole assembly to push the probe into the undrilled sediment. Resistance measured by the thermistor probe when inserted in the sediment is converted via an onboard computer program into a series of temperature-versus-time graphs (e.g., Site 760 chapter, Fig. 33).

After an initial heating due to probe insertion, the temperature records commonly decay towards an equilibrium which approximates the *in-situ* temperature. This equilibrium may represent either an increase or decrease in the initial temperature after insertion. The temperature is estimated by extrapolating to infinity (Erickson, 1984); if this simple relationship does not exist, the temperature has probably not been correctly recorded. Temperature data acquired in this manner may then be plotted against depth to derive a temperature gradient (e.g., Site 763 chapter, Fig. 39). Finally, a heat-flow value (the rate at which heat escapes from an area of the earth's surface) is calculated by multiplying the thermal gradient by the thermal conductivity.

REFERENCES

Aita, Y., 1987. Middle Jurassic to Lower Cretaceous radiolarian biostratigraphy of Shikoku with reference to selected sections in Lombardy Basin and Sicily. *Sci. Rep. Tohoku Univ., Ser. 2*, 58.

Banner, F. T. and Blow, W. H., 1965. Progress in the planktonic foraminiferal biostratigraphy of the Neogene. *Nature*, 208:1164–1166.

Baumgartner, P. O., 1984. A Middle Jurassic–Early Cretaceous low-latitude radiolarian zonation based on unitary associations and age of Tethyan radiolarites. *Eclogae Geol. Helv.*, 77:729–836.

Berggren, W. A., 1969. Cenozoic chronostratigraphy, planktonic foraminiferal zonation and the radiometric time scale. *Nature*, 224:1072–1075.

Berggren, W. A., and Miller, K. G., 1988. Paleogene tropical planktonic foraminiferal biostratigraphy and magnetostratigraphy. *Micropaleontology*, 34:362–380.

_____, in press. Cenozoic bathyal and abyssal calcareous benthic foraminiferal zonation. *Micropaleontology*.

Biquand, D. and Prévot, M., 1970. Sur la surprenante résistance a la destructon par champs magnétiques alternatifs de l'aimantation rémanente visqueuse acquise par certaines roches sédimentaires au cours d'un séjour, même bref, dans le champ magnétique terrestre. *C.R. Acad. Sci., Ser 2*:270:363–365.

Blow, W. H., 1969. Late middle Eocene to Recent planktonic foraminiferal biostratigraphy. *In* Brönnimann, P. and Renz, H. H. (Eds.), *Proc. 1st Intl. Conf. Planktonic Microfossils.*, 1: 199–422.

_____, 1979. *The Cainozoic Globigerinida* (3 Vols.): Leiden, (E. J. Brill).

Boyce, R. E., 1976. Definitions and laboratory techniques of compressional sound velocity parameters and wet-water content, wet-bulk density, and porosity parameters by gravimetric and gamma ray attenuation techniques. *In* Schlanger, O. S., Jackson, E. D., et al., *Init. Repts. DSDP*, 33: Washington (U.S. Govt. Printing Office), 931–958.

_____, 1977. Deep Sea Drilling Project procedures for shear strength measurements of clay sediments using modified Wykeham-Farrance laboratory vane apparatus. *In* Barker, P. E., Dalziel, I.W.D., et al., *Init. Repts. DSDP*, 36: Washington (U.S. Govt. Printing Office), 1059–1068.

Bralower, T. J., 1987. Valanginian to Aptian calcareous nannofossil stratigraphy and correlation with the upper M-sequence magnetic anomalies. *Mar. Micropaleontol.*, 11:293–310.

Bralower, T. J., Monechi, S., and Thierstein, H. R., 1989. Calcareous nannofossil zonation of the Jurassic-Cretaceous boundary interval and correlation with the geomagnetic polarity timescale. *Mar. Micropaleontol.*, 14:153–235.

Brown, L. F., and Fisher, W. L., 1977. Seismic stratigraphic interpretation of depositional systems. *In* Payton, C. E. (Ed.), *Seismic stratigraphy—Applications to hydrocarbon exploration:* AAPG Mem., 26:213–248.

Caron, M., 1985. Cretaceous planktonic foraminifera. *In* Bolli, H. M., Saunders, J. B., and Perch-Nielsen, K. (Eds.), *Plankton Stratigraphy:* Cambridge (Cambridge Univ. Press), 17–86.

Carter, D.J.T., 1980. *Echo-Sounding Correction Tables (Formerly Matthews' Tables):* Taunton, U.K., (Hydrographic Dept., Ministry of Defence).

Channell, J.E.T., Freeman, R., Heller, F. and Lowrie, W., 1982. Timing of diagenetic haematite growth in red pelagic limestones from Gubbio (Italy). *Earth Planet. Sci. Lett.*, 58:189–201.

Dailey, D. H., 1983. Late Cretaceous and Paleocene benthic foraminifers from Deep Sea Drilling Project Site 516, Rio Grande Rise, western South Atlantic Ocean. *In* Barker, P. F., Carlson, R. L., and Johnson, D. A. et al., *Init. Repts. DSDP*, 72: Washington (U.S. Govt. Printing Office), 757–782.

Dunham, R., 1962. Classification of carbonate rocks according to depositional texture. *In* Ham, W. E. (Ed.), *Classification of Carbonate Rocks*: Tulsa (AAPG), 108–121.

Emeis, K.-C., and Kvenvolden, K. A., 1986. Shipboard Organic Geochemistry on *JOIDES Resolution*. *ODP Tech. Note*, 7.

Erickson, A. J., 1984. Theory, techniques and interpretation of downhole temperature measurements. *In* Heath, G. R. (Ed.), *Sedimentology, Physical Properties, and Geochemistry in the Initial Reports of the Deep Sea Drilling Project Volumes 1–44: An Overview*. World Data Center A for Geology and Geophysics, Report MGG-1.

Espitalie, J., Deroo, G., and Marquis, F., 1985. *Rock Eval Pyrolysis and Its Applications:* Rueil Malmaison (Inst. Fr. Pet.).

Espitalie, J., Laporte, J. L., Madec, M., Marquis, F., Leplat, P., and Paulet, J., 1977. Methode rapide de caracterisation des roches mere, de leur potentiel petrolier et de leur degre d'evolution. *Rev. Inst. Fr. Pet.*, 32:23–43.

Fisher, R. V., and Schmincke, H.-U., 1984. *Pyroclastic Rocks:* Berlin (Springer-Verlag).

Galbrun, B., Gabilly, J., and Rasplus, L., 1988. Magnetostratigraphy of the Toarcian statotype sections at Thouars and Airvault (Deux-Sèvres, France). *Earth Planet. Sci. Lett.*, 87:453–462.

Gartner, S., 1977. Calcareous nannofossil biostratigraphy and revised zonation of the Pleistocene. *Mar. Micropaleontol.*, 2:1–25.

Gieskes, J. M., 1974. Interstitial water studies, Leg 25. *In* Simpson, E.S.W., Schlich, R., et al. *Init. Repts. DSDP*, 25: Washington, (U.S. Govt. Printing Office), 361–394.

Gieskes, J. M., and Peretsman, G., 1986. Procedures of interstitial water analysis. *ODP Tech. Note*, 5.

Haq, B. U., Hardenbol, J., and Vail, P. R. 1987. Chronology of fluctuating sea-levels since the Triassic. *Science,* 235:1156–1167.

_____, 1988. Mesozoic and Cenozoic chronostratigraphy and cycles of sea level change. *In* Wilgus, C., et al. (Eds.), *Sea-level change—An Integrated Approach*, Soc. Econ. Paleontol. Mineral. Spec. Publ., 42:71–108.

Hedberg, H. D. 1976. *International Stratigraphic Guide:* New York (Wiley, New York).

Helby, R., Morgan, R., and Partridge, A. D., 1987. A palynological zonation of the Australian Mesozoic. *Mem. Assoc. Australas. Palaeontol.,* 4:1–94.

Kvenvolden, K. A., and Barnard, L. A., 1983. Gas hydrates of the Blake Outer Ridge, Site 533, Deep Sea Drilling Project Leg 76. *In* Sheridan, R. E., Gradstein, F. M., et al., *Init. Repts. DSDP*, 76, Washington: (U.S. Govt. Printing Office), 353–365.

Kvenvolden, K. A., and McDonald, T. J., 1985. Gas hydrates in slope sediments of the Middle America Trench, DSDP Leg 84. *In* Von Huene, R., Aubouin, J., et al., *Init. Repts. DSDP*, 84, Washington: (U.S. Govt. Printing Office), 667–682.

Lee, H. J., 1984. State of the art: laboratory determination of strength of marine soils. *In* Chaney, R. C., and Demars, K. R. (Eds.), *Strength Testing of Marine Sediments: Laboratory and In-situ Measurements*, ASTM Spec. Tech. Publ. 883, 181–250.

Lowrie, W., and Heller, F., 1982. Magnetic properties of marines limestones. *Rev. Geophys. Space Phys.*, 20:171–192

Manheim, F. T., and Sayles, F. L., 1974. Composition and origin of interstitial waters in marine sediments, based on deep sea drill cores. *In* Goldberg, E. D. (Ed.), *The Sea* (Vol. 5): New York (Wiley), 527–568.

Manheim, F. T., and Waterman, L. S., 1974. Diffusimetry (diffusion constant estimation) on sediment cores by resistivity probe. *In* von der Borch, C. C., Schlater, J. C., et al., *Init. Repts. DSDP*, 22: Washington (U.S. Govt. Printing Office), 663–670.

Martini, E., 1971. Standard Tertiary and Quaternary calcareous nannoplankton zonation. *In* Farinacci A. (Ed.), *Proc. 2nd Planktonic Conf.:* Rome (Ed. Tecnoscienza), 739–785.

Mazzullo, J. M., Meyer, A., and Kidd, R., 1988. New sediment classification scheme for the Ocean Drilling Program. *In* Mazzullo, J. M. and Graham, A. G. (Eds.), *ODP Tech. Note*, 8.

Moullade, M., 1984. Jnteret des petits Foraminiferes benthiques "profonds" pour la biostratigraphic et l'analyse des paleoenvironnements oceaniques mesozoiques. *In* Oertli, H. J. (Ed.), *2nd Inter. Symp. Benth. Foraminifera,* 429–464.

Munsell Soil Color Charts, 1971. Baltimore (Munsell Color).

Pessagno, E. A., Jr., 1976. Radiolarian Zonation and Stratigraphy of the Upper Cretaceous portion of the Great Valley Sequence, California Coast Ranges. *Micropaleontology, Spec. Publ.,* 2.

Posamentier, H., Jervey, M. T., and Vail, P. R., 1988. Eustatic control on clastic deposition I-Conceptual Framework. *In* Wilgus, C., et al. (Eds.), *Sea-level change—An Integrated Approach*, Soc. Econ. Paleontal. Mineral., Spec. Publ., 42:109–124.

Riedel, W. R., and Sanfilippo, A., 1978. Stratigraphy and evolution of tropical Cenozoc radiolarians. *Micropaleontology,* 23:61–96.

Roth, P. H., 1978. Cretaceous nannoplankton biostratigraphy and oceanography of the Northwestern Atlantic Ocean. *In* Benson, W. E., Sheridan, R. E., et al., *Init. Repts. DSDP*, 44: Washington (U.S. Govt. Printing Office), 731–759.

Roth, P. H., and Thierstein, H. R., 1972. Calcareous nannoplankton, Leg 14 of the DSDP. *In* Hayes, D. E., Pimm, A. C., et al., *Init. Repts. DSDP*, 14: Washington (U.S. Govt. Printing Office), 421–485.

Sanfilippo, A., and Riedel, W. R., 1985. Cretaceous Radiolaria. *In* Bolli, H. M., Saunders, J. B., and Perch-Nielsen, K. (Eds.), *Plankton Stratigraphy:* Cambridge (Cambridge Univ. Press), 573–630.

Sanfilippo, A., Westberg-Smith, M. J., and Riedel, W. R., 1985. Cenozoic Radiolaria. *In* Bolli, H. M., Saunders, J. B., and Perch-Nielsen, K. (Eds.), *Plankton Stratigraphy:* Cambridge (Cambridge Univ. Press, 631–712.

Schaaf, A., 1981. Late Early Cretaceous radiolaria from Deep Sea Drilling Project Leg 62. *In* Thiede, J., Vallier, T. L., et al., *Init. Repts. DSDP*, 62: Washington (U.S. Govt. Printing Office), 419–470.

_____, 1984. Les Radiolaires du Cretace Inferiuer et Moyen: Biologie et Systematiques. *Sci. Geol. Mem.,* 75.

Schott, M., 1984. Mikrofaziell-mutivariate Analyse einer rhäto-liassischen Karbonatplattform in den Nördlichen Kalkalpen. *Facies,* 11:229–280.

Shepard, F., 1954. Nomenclature based on sand-silt-clay ratios. *J. Sediment. Petrol.*, 24:151–158.

Sissingh, W., 1977. Biostratigraphy of Cretaceous calcareous nannoplankton. *Geol. Mijnbouw,* 56:37–65.

Shipboard Scientific Party, 1989. Explanatory Notes. *In* Pierce, J., Weissel, J., et al., *Proc. ODP, Init. Repts.,* 121: College Station, TX (Ocean Drilling Program), 33–62

Sliter, W. V., 1977. Cretaceous foraminifers from the southwestern Atlantic Ocean, Leg 36, Deep Sea Drilling Project. *In* Barker, P. F., Dalziel, I.W.D., et al., *Init. Repts. DSDP*, 36: Washington (U.S. Govt. Printing Office), 269–492.

Taketani, Y., 1982. Cretaceous radiolarian biostratigraphy of the Urakawa and Obira areas, Hokkaido: *Sci. Rep. Tohoku Univ., Ser 2,* 52.

Thierstein, H. R., 1971. Tentative Lower Cretaceous nannoplankton zonation. *Eclogae. Geol. Helv.,* 64:458–488.

_____, 1973. Lower Cretaceous calcareous nannoplankton zonation. *Abh. Geol. Bundesanst. Austria,* 29:1–52.

Vacquier, V., 1985. The measurement of thermal conductivity of solids with a transient linear heat source on the plane surface of a poorly conducting body. *Earth Planet. Sci. Lett.*, 74:275–279.

Van Morkhoven, F.P.C.M., Berggren, W. A., and Edwards, A. S., 1986. *Cenozoic Cosmopolitan Deep-water Benthic Foraminifera.* Bull. Cent. Rech. Explor. Prod Elf-Aquitaine, Mem. 11.

Van Wagoner, J. C., Posamentier, H. W., Mitchum, R. M., Vail, P. R., Sorg, J. F., Loutit, T. S., and Hardenbol, J., 1988. An overview of the fundamentals of sequence stratigraphy and key definitions. *In* Wilgus, C., et al. (Eds.), *Sea-level Change—An Integrated Approach*, Soc. Econ. Paleontal. Mineral., Spec. Publ., 42:39–46.

Von Herzen, R. P., and Maxwell, A. E., 1959. The measurment of thermal conductivity of deep-sea sediments by a needle probe method. *J. Geophys. Res.*, 65:1557–1563.

Wentworth, C. K., 1922. A scale of grade and class terms for clastic sediments. *J. Geol.*, 30:377–392.

Yamasaki, T., 1987. Radiolarian assemblages of the Izumi Group in Shikoku and western Awayi Island, Southwest Japan. *Chishitsugaku Zasshi,* 93:403–417.

Zaninetti, L., 1976. Les Foraminifères du Trias. *Riv. Ital. Paleontol., 82:1–258.*

Ms 122A-104